Altered neutrophil extracellular traps in response to *Mycobacterium tuberculosis* in persons living with HIV with no previous TB and negative TST and IGRA

Authors: EE Kroon[1*], W Correa-Macedo[2,3,4], R Evans[5,6], A Seeger[7], L Engelbrecht[8], JA Kriel[8], B Loos[9], N Okugbeni[1,10], M Orlova[2,3,4], P Cassart[2,3], CJ Kinnear[1,10], GC Tromp[1], M Möller[1], RJ Wilkinson[7,11,12], AK Coussens[7,5,6], E Schurr[2,3,4] and EG Hoal[1].

[1] DSI-NRF Centre of Excellence for Biomedical Tuberculosis Research; South African Medical Research Council Centre for Tuberculosis Research; Division of Molecular Biology and Human Genetics, Faculty of Medicine and Health Sciences, Stellenbosch University, Cape Town, South Africa.

[2] Program in Infectious Diseases and Immunity in Global Health, The Research Institute of the McGill University Health Centre, 1001 boul Décarie, Site Glen Block E, Room EM3.3210, Montréal, QC H4A3J1, Canada

[3] McGill International TB Centre, McGill University, Montréal, QC, Canada

[4] Department of Biochemistry, McGill University, Montréal, QC, Canada

[5] Infectious Diseases and Immune Defence Division, Walter and Eliza Hall Institute of Medical Research, Parkville, VIC,3052, Australia

[6] Department Medical Biology (WEHI), Faculty of Medicine, Dentistry and Health Sciences, University of Melbourne, Parkville, VIC,3052, Australia

[7] Wellcome Centre for Infectious Diseases Research in Africa, Institute of Infectious Disease and Molecular Medicine and Department of Medicine, University of Cape Town, Observatory 7925, South Africa

[8] Central Analytical Facilities, Microscopy Unit, Stellenbosch University, Cape Town, South Africa

[9] Department of Physiological Sciences, Stellenbosch University, Stellenbosch 7600, South Africa

[10] South African Medical Research Council Genomics Platform, Tygerberg 7505, South Africa

[11] Department of Infectious Diseases, Imperial College London, W12 0NN, United Kingdom

[12] The Francis Crick Institute, London, NW1 1AT, United Kingdom

* Corresponding author

Email: elouise_k@sun.ac.za

Abstract

Persons living with HIV (PLWH) have an increased risk for tuberculosis (TB). After prolonged and repeated exposure, some PLWH never develop TB and test persistently negative in tests of immune sensitization tuberculin skin test (TST) and interferon gamma release assays (IGRA) for *Mycobacterium tuberculosis* (*Mtb)*. This group has been identified and defined as HIV+ persistently TB, tuberculin and IGRA negative (HITTIN). To investigate potential innate mechanisms unique to individuals with the HITTIN phenotype we compared their neutrophil *Mtb* infection response to that of PLWH, with no TB history, but who test persistently IGRA positive, and tuberculin positive (HIT). Neutrophil samples from 17 HITTIN (PMN_{HITTIN}) and 11 HIT (PMN_{HIT}) were isolated and infected with *Mtb* H37Rv for 1h and 6h. RNA was extracted and used for RNAseq analysis. At 1h of *Mtb* infection, PMN_{HITTIN} displayed 151 significantly upregulated and 40 significantly downregulated differentially expressed genes (DEGs) and PMN_{HIT} 98 significantly upregulated and 11 significantly downregulated DEGs. At the 6h timepoint, PMN_{HITTIN} displayed 3106 significantly upregulated and 3548 significantly downregulated DEGs while PMN_{HIT} had 3816 significantly up- and 3794 significantly downregulated DEGs. There was no significant differential transcriptional response at 1h between infected PMN_{HITTIN} and $PMN_{HIT.}$ However, when contrasting the log_2FC 6h infection response to *Mtb* from PMN_{HITTIN} against PMN_{HIT}, 2285 genes showed significant differential response between the two groups. Apoptosis and NETosis were key pathways linked to the enrichment of genes in PMN_{HITTIN} when contrasted to PMN_{HIT} after 6h infection with *Mtb*. Fluorescence microscopy revealed relatively lower neutrophil extracellular trap formation and cell loss in PMN_{HITTIN} compared to PMN_{HIT}, showing that PMN_{HITTIN} have a distinct response to *Mtb*.

Introduction

Worldwide, tuberculosis (TB) remains the leading cause of death by a single bacterial agent (1). People who are living with HIV (PLWH) have an increased risk of TB (2,3). We previously identified a cohort of PLWH, living in a community with high TB burden in the Western Cape, South Africa, who are persistently TB, tuberculin skin test (TST) and interferon gamma release immune assay (IGRA) negative (HITTIN) (4–6). TST and IGRA measure persistent adaptive immune memory to *Mycobacterium tuberculosis* (*Mtb)* protein antigens and are used as a surrogate for prior *Mtb* infection. Despite these persons having a history of previously low CD4+ T-cell counts, prior to antiretroviral therapy (ART), they display no canonical evidence of prior *Mtb* infection or history of disease (4). However, we

did detect circulating *Mtb*-specific antibodies, despite absence of canonical T-cell memory to dominant *Mtb* antigens, suggesting these individuals may possess a unique immune mechanism of TB protection, not reliant on conventional T-cell help.

We hypothesized that the innate immune system, and specifically neutrophils, play an inherent role in the protective control of *Mtb* infection in HITTIN. Neutrophils are the most abundant leukocytes and among the first responders to *Mtb* infection in the lung in animal models as well as humans (7). They are armed with an arsenal of antimicrobial granules known to restrict *Mtb* growth and are key players in the inflammatory response against *Mtb* (8–11). Neutrophils can control *Mtb* growth during acute infection (8,11,12). Household pulmonary TB contacts with higher initial peripheral neutrophil counts were less likely to become infected with *Mtb* (11). Despite lower RNA expression in neutrophils (PMN) compared to other innate immune cells, pathogen-triggered gene expression changes underlie microbial responses by PMN (13,14).

The mechanism of cell death can influence the outcome of *Mtb* infection control. Neutrophils control inflammation, predominantly through apoptotic and cell clearance mechanisms with efferocytosis of *Mtb*-infected apoptotic neutrophils by macrophages favoring a beneficial host outcome (14–18). Neutrophil extracellular traps (NETs) were recently highlighted as a potentially important mechanism of resistance to TST/IGRA conversion in a Ugandan cohort (19). As a primary cell death effector mechanism, neutrophils decondense their chromatin following histone modification, unraveling their DNA, which is then coated in cytoplasmic granular proteins before the DNA/histone/protein complex is expelled from the lysing neutrophil. This released web-like structured NET is able to capture extracellular microbes and kill them using the attached granule-derived antimicrobial peptides and histones (20,21). *Mtb*-induced NETs are phagocytosis and reactive oxidative species (ROS) dependent, but have been suggested to lack *Mtb* microbicidal activity (22,23). Recent studies point to potential crosstalk of NETs and forms of necrotic cell death pathways such as pyroptosis, despite the classical definition of NETosis as a unique mechanism of cell death (24). Necrotic neutrophil cell death, uncontrolled type 1 interferon (IFN) responses and abundant ROS drive a hyperinflammatory neutrophil phenotype and contribute to TB severity (18,25–28).

The aim of this study was to gain insight into mechanisms underlying early neutrophil responses to *Mtb* in HITTIN persons with apparent protection from *Mtb* infection as inferred from the absence of canonical T-cell memory. Specifically, we tested if neutrophils from HITTIN study participants (PMN_{HITTIN}) displayed a transcriptional response to *Mtb* infection that was significantly different from that found in neutrophils from PLWH who have a robust

Mtb-specific T-cell response, testing persistently TST and IGRA positive, but also with no history of TB (HIT). We demonstrated that the *in vitro Mtb*-induced gene expression changes in neutrophils from the HITTIN and HIT participants were significantly different. Genes differentially regulated by *Mtb* between the two groups were enriched for key regulators of ROS and NET formation. Fluorescence microscopy images corroborated the transcriptomic findings with PMN_{HIT} demonstrating a greater response to *Mtb* with more NETs forming after infection. PMN_{HITTIN} responded with less NETs and lower counts of key genes associated with nicotinamide adenine dinucleotide phosphate hydrogen (NADPH) activity and ROS formation possibly contributing to greater effector control of *Mtb*.

Results

Study participants and samples

Individuals included in the HITTIN and HIT groups were a part of the large ResisTB cohort (4). Neutrophils obtained from 17 HITTIN and 11 HIT individuals, all PLWH and established on ART, were used in the final analysis (Table 1). These samples were part of stringently defined and highly selected groups who are PLWH, living in a high TB burden community, with previously low CD4+ counts prior to ART, yet never developed TB.

The average age of participants in the HITTIN group was 43.71 (±6.43) years and that of HIT was 44.09 (±6.89) (Table 1). There were no significant differences between the ratio of females to males in each group (p=0.6, Fisher's exact test), age (p=0.9, Wilcoxon rank sum test), or BMI (p=0.6, Wilcoxon rank sum test) of the participants. All but one participant had CD4+ counts of < 200 cells/mm^3 prior to starting ART. Participants had controlled viral loads. One participant was on isoniazid *Mtb* prophylactic therapy (IPT) at the time of the enrolment, this was corrected for during the analysis. All PLWH receive IPT according to national guidelines in South Africa. There was no significant difference between the groups in terms of having taken prior IPT and time spent on IPT (p=0.2, Fisher's exact test). HITTIN and HIT have a similar distribution of chronic disease (p=0.4, Fisher's exact test), and social habits such as cigarette smoking (p=0.5, Fisher's exact test), alcohol use (p=0.2, Fisher's exact test) and cannabis use (p=0.4, Fisher's exact test).

Gene expression analysis showed a strong transcriptional response of PMN to *Mtb* in HITTIN and HIT

Neutrophils were isolated from whole blood and infected with *Mtb* H37Rv for 1h and 6h. Purity of isolated neutrophils was confirmed by flow cytometry, with similar proportions of CD45+CD15+CD66b+CD16+ neutrophils isolated for HITTIN and HIT individuals (p=0.28, Wilcoxon rank sum test) (S1 and S2 Tables). RNA was extracted from uninfected and infected neutrophils (PMN) at 1h and 6h timepoints and differential gene expression analyses performed by RNAseq. Significant differentially expressed genes (DEGs) were defined by an absolute cutoff of a log2FC of 0.2 and a false discovery rate (FDR) adjusted p-value of 5% (Table 2, S3 Table).

Mtb infection triggered significant gene expression changes when compared to uninfected PMN at 1h: 151 up- and 40 downregulated genes for PMN_{HITTIN} while 98 genes were up- and 11 were downregulated for PMN from the HIT group (PMN_{HIT}) (Figs 1A and B, S3 Table). A higher number of *Mtb* activated gene expression changes were observed at 6h post infection compared to 6h uninfected with 3106 up- and 3548 downregulated DEGs for HITTIN and 3816 up- and 3794 downregulated DEGs for HIT (Figs 1D and E, S3 Table).

Differential gene expression analysis showed a lower overall fold change difference during *Mtb* infection of PMN from HITTIN compared to HIT

Given the high number of DEGs at 6h for both PMN_{HITTIN} and PMN_{HIT} we next compared the overall difference in transcriptomic response to *Mtb* between the two PMN groups. Consistent with different numbers of DEGs identified for each phenotypic group, when we evaluated the statistical significance of expression changes between the HITTIN and HIT groups, we identified an overall dampened 6h transcriptomic response in PMN_{HITTIN} compared to PMN_{HIT} (Fig 2). Next, by correlating the expression changes of up- and downregulated DEGs, identified for each PMN infection phenotype, we observed that differential expression across phenotypes was correlated with the log_2FC. Despite differences in log_2FC between groups, we observed a strong correlation of log_2FC values between groups after 6h infection (R = 0.96) whilst the 1h correlation was weaker (R = 0.75) (Fig 3).

When comparing transcriptional responses of infected PMN_{HITTIN} and PMN_{HIT} directly, no significant DEG were identified at the log_2FC cutoff of 0.2 with FDR < 0.05, at 1h (Fig 1C). However, contrasting the log_2FC from PMN_{HITTIN} against PMN_{HIT}, at 6h post *Mtb* infection, we identified 2285 genes with significant differential response between the two groups (Fig 1F).

Since the 1h time point showed limited differences in gene induction by *Mtb*, we focused on the 6h time point differences between PMN phenotypes in subsequent analyses. Irrespective of up- or downregulation of specific genes, the absolute response to *Mtb* after 6h was always smaller in PMN_{HITTIN}.

Pathway and Gene Ontology (GO) enrichment analysis for DEGs between PMN_{HITTIN} and PMN_{HIT} after 6h *Mtb* infection

We next investigated the 2285 genes with significant differential transcriptional response of PMN_{HITTIN} and PMN_{HIT} to *Mtb* after 6 hours infection by examining the different pathways and analyzing the biological processes that are characterized by these genes. We conducted separate term enrichment analyses of up- and downregulated genes and a third analysis that considered both up- and downregulated genes. GO terms and Kyoto Encyclopedia of Genes and Genomes (KEGG) and Reactome pathways were considered significant if a term was enriched for at least 5 DEGs and a FDR cutoff of 10%. An overview of the results is shown in Table 2. By focusing on all DEGs significantly different between PMN_{HITTIN} and PMN_{HIT}, we observed a total of 496 enriched KEGG, Reactome and GO terms (Table 2). When evaluating genes more strongly triggered in PMN_{HITTIN} we detected 29 terms. Conversely, when focusing on genes less strongly triggered in PMN_{HITTIN} and comparatively to PMN_{HIT}, we detected 719 terms (Table 2).

Manhattan plots for the three term analyses at 6h are shown in Fig 4 with significantly different terms and pathways of interest indicated. Amongst the enriched terms in PMN_{HITTIN}, were “Apoptosis”, “Neutrophil extracellular trap formation”, and “NADPH regeneration”, which are terms that directly relate to a possible increased microbicidal activity of PMN_{HITTIN} (Fig 4). By comparison, terms with genes triggered relatively less strongly in PMN_{HITTIN} compared to PMN_{HIT} were dominated by genes involved in neutrophil chemotaxis, neutrophil degranulation, necroptosis and necrotic death (Fig 4 C). We focused on the DEGs associated with the “Neutrophil extracellular trap formation” pathway in KEGG and followed this by functional verification using fluorescent microscopy to evaluate the biological outcome in the total amount of NETs observed between HITTIN vs HIT (Table 3).

DEGs in HITTIN vs HIT after 6h *Mtb* infection in the “Neutrophil extracellular trap formation” pathway

As the major functional pathway of interest, we next investigated the DEGs associated with the "Neutrophil extracellular trap formation" enriched in the combined KEGG pathway (Fig 4A, Table 3). Compared to PMN_{HIT}, *Mtb* infection of PMN_{HITTIN}, triggered a lower upregulation of genes involved in the multiple-protein NADPH oxidase complex including *Rac family small GTPase 2* (*RAC2)*, and the transmembrane catalytic [cytochrome b-245 - alpha (*CYBA*) and -beta (*CYBB*)]. NADPH oxidase Nox2 (NOX2, encoded by *CYBB*) oxidizes NADPH and is one of the multiple cellular processes required for ROS production and NET formation (29–31). *CYBB* is a nuclear factor kappa B (NF-κB) transcriptional target and together with *NFKB1* was also less upregulated in PMN_{HITTIN}. Interestingly, *NCF2*, the gene encoding neutrophil cytosolic factor 2 (NCF-2 or p67-phox) was downregulated in PMN_{HITTIN} and upregulated in PMN_{HIT}. PMN_{HITTIN}, also showed enrichment for DEGs related to "NADPH regeneration" (Fig 4B). NADPH can dually aid in ROS detoxification or production and is key for ROS mediated NET formation (30,32,33).

Histone deacetylases (HDACs) play a key role in NET formation and allow for peptidylarginine deiminase 4 (PAD4) mediated histone citrullination the initial step in chromatin decondensation (34,35). Compared to $PMN_{HIT,}$ PMN_{HITTIN} had a less downregulated response in *HDAC1*, *HDAC3, HDAC4* and *PADI4* at 6h of *Mtb* infection. *Gasdermin D* (*GSDMD*) which plays a key role perforating the nuclear membrane to aid release of the decondensed chromatic during NET formation (36,37), also displayed the same pattern of expression regulation. *Caspase 1* (*CASP1*) and *4* (*CASP4*) which activate GSDMD have a lower upregulation in PMN_{HITTIN} compared to PMN_{HIT} after 6h *Mtb* infection (38).

Other DEGs enriched in the KEGG NET pathway, are also involved in additional neutrophil functional responses. Cell membrane receptors *TLR2* and *TLR4* were less upregulated in PMN_{HITTIN} in response to 6h *Mtb* infection. Downstream of TLR4, pathway activation of NF-κB, Protein Kinase B (AKT) and phosphoinositide 3-kinase (PI3-K) lead to pro-survival mechanisms (39). Integral to this TLR signaling system is mitogen-activated protein kinase (MAPK) and PI3-K. Dysregulation in especially the PI3-K/AKT signaling system contributes to an imbalance in neutrophil chemotaxis and can heighten inflammation and decrease pathogen clearance (40,41). *MAP2K2* was less upregulated while *MAPK1, MAPK3, AKT1, AKT2* and *PIK3CD* were less downregulated in PMN_{HITTIN}. Azurocidin 1 (*AZU1*), the only antimicrobial peptide gene also included in the NET term, was downregulated after 6h *Mtb* infection in PMN_{HITTIN} whilst upregulated in infected PMN_{HIT} (Table 3).

NET area change difference between HITTIN and HIT from 1 to 6h after *Mtb* infection

Finally, to functionally validate whether the differential NET-associated DEGs response between PMN_{HITTIN} and PMN_{HIT} resulted in a difference in NET formation, we used fluorescent microscopy to quantify the area of NETs induced at 1h and 6h infection, as well as the remaining nuclei. We stained fixed cells which were processed in parallel with the cells used for RNAseq. NETs were stained using anti-H2AH2B/DNA (PL2-3) which detects decondensed chromatin and nuclear DNA stained with Hoechst, and the area of both features was quantified.

As a measure of cellular viability over time we compared the total change in cell nuclei area between cells fixed at 1h and 6h of infection with *Mtb.* There was no significant two way interaction between PMN_{HITTIN} and PMN_{HIT} and the infection status, $F(1,12)=1.1870$, $p=0.30$, including a similar trend in direction of response for both PMN. However, there was a significant *Mtb* infection effect, $F(1,12)=9.7290$, $p=0.009$, with pairwise comparisons showing a significantly greater decrease in total cell nuclei area between 1h and 6h after *Mtb* infection for PMN_{HIT} compared to PMN_{HITTIN} ($p=0.04$, pairwise t-test) (Fig 5 and S1 Fig).

When then comparing difference in NET area at 1h vs 6h, there was a statistically significant interaction between the PMN groups and infection status, $F(1, 10.5924) = 5.3398$, $p < 0.0421$). The simple main effect of phenotype group, considering the Bonferroni adjusted p-value was significant for *Mtb* infection ($p=0.0007$), but not for non-infection ($p=1$). Consistent with the greater viability of PMN_{HITTIN} at 6h of infection, pairwise comparisons show that PMN_{HITTIN} also induce a significantly smaller change in NETs produced between 1h and 6 h of infection, compared to PMN_{HIT} ($p=0.0003$) (Fig 5 and S1 Fig).

Discussion

HITTIN remain persistently TST, IGRA and TB negative despite prolonged *Mtb* exposure and antibody evidence of prior infection. This suggests HITTIN have different protective mechanisms in the early response to *Mtb* infection to that which occurs in HIT who convert to a positive TST and IGRA following *Mtb* infection. Here we investigated the DEGs of PMN_{HITTIN} to determine whether they are a distinct and previously undefined group that contribute to HITTINs unique ability to control *Mtb* infection, prevent progression to TB, and interact with the adaptive immune response while possibly limiting persisting *Mtb*-specific IFN-γ T-cell memory responses. Using RNAseq analysis of *ex vivo Mtb* infected PMN we

found that PMN_{HITTIN} had an overall lower transcriptional FC response to *Mtb* after 6h of infection relative to $PMN_{HIT.}$ Positively enriched terms and pathways included apoptosis, NETosis, NADPH regeneration and ROS formation, with pathways related to necrotic cell death, necroptosis, neutrophil chemotaxis, degranulation and immune exhaustion which were triggered less strongly in PMN_{HITTIN} compared to PMN_{HIT} after 6h infection with *Mtb*. Using fluorescence microscopy, we demonstrate that after 6h of infection PMN_{HITTIN} have undergone less NETosis than $PMN_{HIT,}$ corroborating the overall lower transcriptional response to *Mtb* infection after 6h seen in PMN_{HITTIN}. The question arises whether the less pronounced response by PMN_{HITTIN} facilitates rapid *Mtb* control and a more contained neutrophil response, thereby preventing overt damage and an exacerbated inflammatory cascade, associated with TB. Their relatively lower induction of genes in response to *Mtb* suggests this is likely, requiring future functional studies for confirmation.

Neutrophil degranulation and NET formation processes were observed 1-6 months prior to persons developing TB and play an important role in *Mtb* infection progression to disease as well as potential lung destruction (42). This highlights the important regulatory mechanism of NET formation by neutrophils in the inflammatory response against *Mtb* infection.

After infection with *Mtb*, *Mtb*-induced ROS, mediated necrosis in neutrophils and decreased the ability of macrophages to control *Mtb* growth (18). Transcription of different groups of genes are regulated by NETosis-specific kinase cascades (43). NETs are triggered by a NADPH/ROS dependent or an independent mechanism through TLR2/TLR4/lipopolysaccharide (LPS) activation (44,45). The multi-protein NADPH oxidase complex consists of multiple subunits (including cytosolic p40-phox, p47phox and p67-phox, as well as the catalytic gp91-phox subunit) and other proteins (transmembrane p22-phox and nucleotide-binding Rac2) and is involved in the process to produce ROS (46). ROS is mostly known to modulate a pro-inflammatory effect, with increased levels positively correlated to higher levels of TNF and a greater control of *Mtb* infection (47). High levels of ROS can be damaging, but at lower levels ROS can mediate an anti-inflammatory effect in mouse neutrophils by inhibiting p-AKT and NF-κβ and inducing apoptosis (48–53). In our data, within the “Neutrophil extracellular trap formation” pathway in KEGG, several significantly under-stimulated genes in the pathway suggest potential relatively lower ROS levels in PMN_{HITTIN} which could account for the relatively lower NET formation after 6h infection with *Mtb*. Another alternative mechanism PMN_{HITTIN} displayed for inflammation control was enrichment of “NADPH regeneration”. NADPH may play a role in neutralizing rather than producing ROS in $PMN_{HITTIN.}$

The lower upregulation of *CYBA*, *CYBB* (aka *NOX2*) as well as *RAC2* in PMN_{HITTIN} could point to a mechanism to decrease ROS formation and prevent or decrease necrosis with consequently lower ROS mediated NET formation. Strikingly, *NCF2* was downregulated in PMN_{HITTIN} and upregulated in PMN_{HIT}. The G allele of *NCF2* rs10911362 is associated with protection against TB in the Western Chinese Han population (54). In another study also investigating Chinese Han persons, a rs3794624 polymorphism in *CYBA* was also linked with decreased TB susceptibility (46,54). PMN_{HITTIN} exhibit an interesting potential *NCF2*-mediated mechanism driving less ROS and NET formation with consequently potentially lower necrotic cell death.

TLR2/4 ROS independent mechanisms could also mediate NET formation. A lower upregulation of *TLR2* and *TLR4* in PMN_{HITTIN} likely balance potential inflammatory effects of NET release with downstream upregulation of apoptosis. NETs can also be triggered by activated CASP1 and ELANE cleaving GSDMD (55). *CASP1* was less up- and *GSDMD* less downregulated in PMN_{HITTIN}. Although NETs have not been shown to control *Mtb* infection, the granular components associated with NETs could contribute (56). Azurocidin 1 (AZU1) can interact with pentraxin 3 (PTX3) to enhance microbial function. The mechanism of this interaction is not known. PTX3 is a soluble pattern recognition receptor with increased levels seen in sepsis and TB (57). *PTX3* was significantly upregulated by *Mtb* infection in both PMN_{HITTIN} and PMN_{HIT} but there was not a statistically significant difference between these. The fact that DEGs for other granule proteins were not identified is likely because they are mostly transcribed in immature neutrophils and this degranulation is reflective of their potentially different action (58–60).

HDAC1 has been implicated as a key regulator of innate immunity in monocytes isolated from HIV negative persons who tested persistently TST negative after household TB exposure (61). HDAC inhibitors in macrophages such as phenylbutyrate improved *Mtb* control (61,62). This inhibition was synergistically improved with vitamin D (62). Less downregulation of *HDAC1* in PMN_{HITTIN} translated into a decreased inflammatory response, with a lower upregulation of genes in the NF-kappa β signaling pathway (Fig 4A and C). This corroborates a more repressive or anti-inflammatory role in PMN_{HITTIN}.

Increased NETs can potentiate local damage due to release of granular components, but NET formation has also been shown to limit inflammation through degradation of chemokines and cytokines (63). This intricate balance is likely maintained by PMN_{HITTIN} which despite an abundance of genes associated with NETs make relatively lower total NETs in response to *Mtb* infection. The formation of NETs itself is likely not problematic as PMN_{HITTIN} could potentially effectively localize and trap *Mtb* through NETs and activate other

innate cells such as macrophages (22). The balance of NETosis with other cell death mechanisms may play an additional role to determine the fate of *Mtb*.

Study limitations

Future work is needed to determine if there is a measured difference in ROS released by PMN_{HITTIN} compared to PMN_{HIT}. In addition, neutrophil *Mtb* killing assays will determine if PMN_{HITTIN} show improved *Mtb* infection clearance. Multiple studies have identified neutrophil subpopulations and it is possible that a specific subpopulation could be driving the response differences we observed (64–66). Flow cytometry for identification of potential subpopulations as well as single cell RNA sequencing would be highly informative.

Conclusion

In general, for TB, neutrophils are mostly linked to hyperinflammatory responses and more severe disease. Here we showed a distinctive gene expression profile for neutrophil responses from HITTIN individuals, who appeared protected from TB despite a lack of canonical *Mtb*-specific T-cell memory. These findings put neutrophils at the forefront of potential innate immune cell mechanisms of *Mtb* infection resistance. They highlight a distinct phenotypic response to *Mtb* in PMN_{HITTIN} compared to neutrophils from persons otherwise defined as sensitized by *Mtb*.

Contrary to *Mtb* inducing necrotic cell death mechanisms as in most neutrophils, DEGs in PMN_{HITTIN} showed decreased transcriptional responses for necrosis, with an enrichment of terms related to apoptotic cell death and NETosis. Fluorescence imaging corroborated significant reduction in NET formation between PMN_{HITTIN} and $PMN_{HIT,}$ likely driven by lower ROS transcriptional pathways with a downregulation of *NCF2*, a key mediator in ROS formation, in PMN_{HITTIN}. These molecular data implicated neutrophils as key effector cells in *Mtb* infection resistance. Further increased understanding of the crucial pathways of *Mtb* infection control highlighted in the study could be harnessed for the development of *Mtb* prevention and treatment strategies.

Materials and Methods

Ethics Statement

The study was approved by the Health Research Ethics Committee of Stellenbosch University (S18/08/175(PhD)). Samples used in this study were leveraged from the ResisTB study. The Health Research Ethics Committee of Stellenbosch University (N16/03/033 and

N16/03/033A) and the Faculty of Health Sciences Human Research Ethics Committee of the University of Cape Town (755/2016 and 702/2017) approved participant recruitment for ResisTB. Additional approval was obtained from the City of Cape Town and Western Cape government for access to the relevant clinics.

Participant recruitment

Samples were collected from 29 participants recruited to the ResisTB study in Cape Town, South Africa. The ResisTB study recruited a group of participants between the ages of 35-60 years old. The recruitment of this group for the ResisTB study has been fully described previously (4). Briefly, the participants had to be living with HIV in an area of high *Mtb* transmission and have no history of previous or current TB. They had to have a history of living with a low CD4+ count (either with two CD4+ <350 cells/mm^3 counts at least 6 months apart or a single CD4+ count <200 cells/mm^3) prior to initiating antiretroviral therapy (ART), and be immune reconstituted on ART for at least one year at time of enrolment with the last CD4+ count >200 cells/mm^3 (4). Exclusion criteria included pregnancy, previous TB, symptoms suggestive of active TB disease, participation in other interventional studies, and any AIDS defining illness in the year prior to enrolment. Participants were seen at three visits. During the enrolment visit, blood samples were taken for an IGRA using the QuantiFERON®-TB Gold Plus (QFT®-Plus) in tube test. For follow up, whole blood was collected in an EDTA tube for Ficoll gradient separation and neutrophil isolation as well as a second IGRA, followed by TST administration with PPD RT23 (Staten Serum Institute). After 3 days the TST reading was taken and participants who tested IGRA negative from the first visit had bloods taken for a third and final IGRA. This ensured that any T-cell response that would be boosted by TST administration would be identified by IGRA to ensure participants with low level T-cell memory were correctly identified.

For this study, samples were leveraged from 17 older HITTIN and 11 HIT participants. Age was used as a surrogate for increased exposure frequency to *Mtb* since most persons are infected with *Mtb* by the age of 30-35 in the Western Cape of South Africa, where the study was conducted (67,68).

Neutrophil isolation

Neutrophils were isolated by Ficoll gradient separation. Whole blood diluted 1:1 with 1x Phosphate buffered saline (PBS, Sigma-Aldrich, USA) was layered over the density gradient separation medium (Histopaque / Ficoll-Paque, Sigma-Aldrich, USA). Cells were centrifuged for 25 minutes at 400 x g. After this, cells were washed twice with 4°C PBS and centrifuged each time at 400 x g for 10 minutes at 4°C. Peripheral blood mononuclear cells were

removed first and then the remaining plasma and Ficoll-Paque layer. A red blood cell (RBC) lysis buffer (component concentrations) was added in a ratio of 1:10 or topped up to 50ml, if a 50 ml centrifuge tube was used, to the remaining bottom layer and incubated for 10 minutes at 4°C. RBC lysis buffer (8% Ammonium chloride [NH_4Cl], 0.8% Sodium bicarbonate [$NaHCO_3$, Sigma-Aldrich, USA] and 0.4% Ethylenediaminetetraacetic acid [EDTA, Sigma-Aldrich, USA]).

After RBC lysis, samples were centrifuged at 400 x g for 10 minutes at 4°C and then washed twice with PBS (4°C) and centrifuged at 400 x g for 10 minutes at 4°C. After the cell count, 1 x 10^7 cells in RPMI-1640 with L-glutamine and sodium bicarbonate (Sigma-Aldrich, USA), were seeded evenly over each row of 3 wells in a 6-well plate cell culture plate (Nest Scientific USA Inc., USA) at 0.33 x 10^7 cells per well for the RNA sequencing experiment and 2 x 10^5 cells per well in a 96-well (M0562, Greiner, Sigma Aldrich, USA) for microscopy. For each participant two 6-well plates (one for each time-point i.e., 1 and 6h, with 3 wells for no infection and 3 wells for *Mtb* infection) were seeded. Cells were incubated for 1h-2h at 37°C and 5% CO_2. An aliquot of remaining neutrophils was fixed with 4% Paraformaldehyde (PFA, cat.no. 43368, Alfa Aesar, USA) and then stored overnight at -80°C before transferred to and stored in liquid nitrogen.

Staining for flow cytometry

The fixed neutrophil aliquots were thawed and washed in Dulbecco's phosphate buffered saline (DPBS, Cat. No. 14190144, Thermo Fisher Scientific, Australia). 1.5 x 10^6 cells per participant were resuspended in surface staining buffer comprised of DPBS + 3% Foetal Bovine Serum (FBS, Cat. No. SFBS-AU, Bovogen Biologicals Pty Ltd, Australia). Fluorescently conjugated antibodies for cell surface staining (Supplementary Table 1) were prepared in Brilliant Stain Buffer (Cat. no. 556349, BD Biosciences, Australia) and incubated with cells in a 96 well plate (Cat. no. COR3894, Corning, In Vitro Technologies Pty Ltd, Australia) for 30 minutes at room temperature. Cells were washed using surface staining buffer, permeabilised using a 10-minute incubation in Perm/Wash Buffer (P/W, cat. no. 554723, BD Biosciences, Australia) and washed once with P/W. The remaining antibodies listed in Supplementary Table 1 were prepared in Brilliant Stain Buffer and incubated with cells in a 96 well plate for 45 minutes at 4°C. Cells were washed twice with P/W and flow cytometry data was acquired using the Cytek Aurora Spectral Flow Cytometer (5 laser, 64 detector configuration). Data was unmixed using SpectroFlo (Version 3.0.3) and analysed using FlowJo (FlowJo 10.8.2) and GraphPad Prism 8.0.1 (see methods section ***Flow data analysis***, S2 Fig). Cell single-stained controls were prepared using the same protocol as experimental samples.

Mycobacterial cultures and neutrophil *in vitro* infection

Mtb single cells stocks for infection were prepared as previously described (62). *Mtb* H37Rv was grown in a liquid culture of Middlebrook 7H9 medium (Difco, Becton Dickinson, USA) with albumin-dextrose-catalase (ADC, Becton Dickinson, USA) and 0.05% Tween-80 (Sigma-Aldrich, USA) at 37°C as a standing culture in a tray and mixed by swirling every few days to disperse clumps for 10 days. After 10 days, a liquid culture of 7H9 ADC, without Tween-80, was inoculated with 1/100th volume of day 10 end-exponential growing phase *Mtb* and incubated in static standing culture, only swirled periodically, at 37°C for 10 days. After this, cultures were centrifuged for 5 minutes at 2500RPM. Glass beads were used to break the pellet after which it was resuspended in PBS. The upper part of the bacterial suspension was harvested and spun for 10 minutes at 1400RPM. Then the upper part of the bacterial suspension was harvested again and mixed with glycerol (5% final volume) and aliquots were stored at -80°C. Aliquots was serial diluted before and after freezing and plated on Middlebrook 7H10 agar (Becton Dickinson, USA) plates with oleic acid-albumin-dextrose-catalase (OADC, Becton Dickinson, USA) for colony forming unit (CFU) determination. Prior to infection, aliquots were thawed at room temperature.

Neutrophils were infected at a multiplicity of infection (MOI) of 1:1 for 1h, and 6h at 37°C under 5% CO_2. For the 3 wells in row 1 of each of the two plates, 1ml was removed from each well (3ml per plate giving a total of 6ml from the two plates). After this 2 x 10^7 *Mtb* H37Rv was added to the 6ml, carefully pipetted to mix and then 1ml (0.33 x 10^7 *Mtb* H37Rv) was returned to each of these wells for infection. For each infection experiment, *Mtb* infection MOI were confirmed by CFU counts of serially diluted inoculum plated on 7H10 OADC agar.

Staining for microscopy

Of the neutrophils isolated from 17 older HITTIN and 11 HIT participants, neutrophils from 12 HITTIN and 10 HIT were plated and stained for microscopy imaging. Cell staining was performed on 2 x 10^5 neutrophils per well for uninfected vs infected with *Mtb* H37Rv for each timepoint 1 and 6h. For each time point (1h, 6h) two wells (A, B) were plated for neutrophils to be infected with *Mtb* and two wells for no infection (C,D). At the designated timepoints the supernatant was discarded and replaced with 4% PFA (cat.no. 43368, Alfa Aesar, USA). The plates were incubated at 4°C for 24h, before removing the plates from the BSL-3. PFA was replaced with PBS and plates stored at 4°C.

For immunofluorescence labelling, wells were stained with 1° [1:500 mouse mAB PL2/3, kindly gifted by Arturo Zychlinsky (nucleosomal complex of Histone 2A, Histone 2B and chromatin)] and 2° antibody cocktail [1:1000 α-mouse-Cy3 (cat.no. 715-166-150, Amersham, UK) and 10µg/ml Hoechst 33342 (cat.no. 14533, Sigma-Aldrich, USA)] (69–71). Prior to staining PBS was removed from all wells and replaced with Perm/Quench Buffer (50mM NH_4Cl, 0.2% saponin in PBS) for a 15-minute incubation period. After removing Perm/Quench, PGAS Buffer (0.2% bovine serum albumin (BSA), 0.02% saponin and 0.02% Azide (NaN_3) was added for a 5-minute incubation. Once the PGAS was removed the 1° antibody cocktail was added and left to incubate overnight at 4°C. The following day the 1° antibody cocktail was discarded, and two washes were completed with PGAS buffer before adding the 2° antibody cocktail and incubating in the dark for 1h at room temperature. The staining was completed by removing the 2° antibody cocktail and completing three washes with PGAS buffer. Each well was filled with PGAS buffer to the brim. The plates were covered with foil and stored at 4°C for imaging.

Image acquisition

Image tile scans were acquired with the Zeiss AxioObserver Z1 microscope, equipped with a Colibri 7 light source for excitation of Hoechst 33342 (cat.no. 14533, Sigma-Alrich) with LED-module 385nm, and Cy3 with LED-module 511nm. A quadruple band pass filter and triple band pass filter were used respectively for detection of Hoechst (wavelength range 412-438nm) and Cy3 (wavelength range 546-564 nm). Images were acquired with a LD A-Plan 40x/0.55 objective as a 6 x 8 tile scan to acquire a total area of 1.21mmx1.21mm (S1 Fig).

Imaging processing

Tiles were stitched together into single images using Zeiss ZenPro software (version 2.6), which were imported into FIJI/ImageJ (version 1.53t). Image tiles were split into separate channels, after which background subtraction (ranging from 50-100 pixels) and Otsu based thresholding was conducted on a per image basis to generate a binarized map of each image. Binary images were further processed by using the binary closing function in FIJI, as well as a top hat filter of 1-2 pixels to remove small non-specific pixels. For the nuclear quantification, an additional watershed function was applied to separate borders more accurately. Thereafter, morphometric data were obtained by specifying the area and circularity ranges of particles to be analysed through the Analyze Particles function in FIJI to determine the total area covered.

Preparation of RNASeq libraries

Uninfected and infected neutrophils ($1x10^7$ cells for each) were lysed with TRIzol (Invitrogen TRIzol Reagent, Fisher Scientific, USA) after 1h and 6h after infection, and stored at -80°C. The miRNeasy kit (Qiagen, Germany) was used for total RNA extraction. One sample per participant and condition was used. RNA integrity (RIN) was assessed with the Agilent 2100 Bioanalyzer (Agilent Technologies, Germany). Samples with RIN >7 were selected for library preparation using TruSeq RNA Library Preparation Kit v2, Set A (Illumina, USA). Samples were sequenced in two batches (S4 Table). Batch 1 was a preliminary test batch for exploratory analysis and to confirm data quality from PMN, consisting of samples from 3 HITTIN (18%) and 4 HIT (36%) participants. This was sequenced as unstranded, 100bp, single-end (SE) on an Illumina HiSeq4000 sequencer at Genome Quebec, Montreal, Canada. Batch 2 with samples from 14 HITTIN (82%) and 7 HIT (64%) participants was sequenced as unstranded, 150bp paired-end (PE) on an Illumina NovaSeq6000 sequencer at Genome Quebec, Montreal, Canada. There was no significant difference in the distribution of the samples used for each batch (p=0.4, Fisher's exact test) (S4 Table).

Quality control and raw data pre-processing

The quality of the raw sequence data was accessed by FastQC (v0.11.5) and MultiQC (72,73). The mean quality of reads was high with the mean sequence quality score (Phred Score) >35 for both batches. Duplicates were observed in both batches. For batch 1, sequenced as single-end reads (SE), we detected a fraction of 0.41-0.63 duplicates which fall within and below the expected range (0.66–0.74) of duplicates according to the Universal Human Reference RNA (UHRR) (74). The fraction of duplicates (0.4-0.61) from batch 2 was much higher than expected (0.087–0.18) for paired-end (PE) reads (74). With single-end reads, fragmentation bias is usually the cause of these duplicates. For both SE and PE, de-duplication is not recommended (74). To minimize bias, duplicates were not removed from either of the batches.

Batch 1 and 2 were combined after read counts were generated. For read count generation the same method was applied to both batches. After initial raw sequence quality check by FastQC, data was filtered and trimmed using HTStream (72,75). The occurrences of rRNA read contamination was counted but not removed and contamination with PhiX, a control in Illumina runs, was removed by hts_SeqScreener (75). Adapters were trimmed with hts_AdapterTrimmer and poly(A) tails were removed with hts_PolyATTrim (75). Any remaining N characters (unassigned bases) were removed with hts_NTrimmer and hts_QWindowTrim for quality trimming the end of the reads (75). Reads less than seventy-five base pairs long were removed by hts_LengthFilter(75).

The genome was indexed using GRCh38.p13 v34 (ENSEMBLE v100) and reads were aligned to the genome with STAR (v2.5.3a) in a bam format (76–78). More than 80% of the reads were uniquely mapped. The reads per gene output files were combined before the final unstranded read counts matrix was extracted for all. The gene read count matrix was input in R (v4.0.3) for further analysis (79). The untransformed and raw count matrix was adjusted for batch effect using ComBat-seq while preserving the signal of the biological variables of interest namely the phenogroups (HITTIN vs HIT), the timepoints and infection (80)(S3 Fig).

Differential gene expression analysis

Raw counts were transformed to counts per million (CPM) and filtered using “filterByExpr” in the edgeR package (81). Briefly, the function kept genes at least 25 read counts or more in at least a minimum of samples (calculated as 70% of the samples in the smallest group). For this dataset genes with a CPM of 1.32 in at least 8 (70% of the smallest group of 11 samples) are retained, leaving 14602/60622 (24%) of the genes for further differential expression analysis (S4 Fig). Normalization scaling factors were generated by “calcNormfactors” in edgeR using the method of trimmed mean of M-values (TMM)(81).

Outlier samples were observed in the multidimensional scaling (MDS) plots (S3 Fig). Instead of removing the outliers, limma’s function “voomWithQualityWeights” allows for variations in samples by taking sample-specific variablity as well as the ‘global intensity-dependent variability trends’ as accounted for by ‘voom’, into consideration (82). The expression matrix was normalized and transformed to log2 CPM and sample specific weights were incorporated with abundance dependent weights using limma’s (v3.46.0) function “voomWithQualityWeights” (82,83) (S5 Fig).

Data exploration

Data was visualized with multidimensional scaling (MDS) plots and principal components analysis (PCA) Scree plot (S6 and S7 Figs). Normalized counts were plotted without covariate correction to examine data for potential covariate effect. Initially clear separation was seen by batch effect, but this was corrected for (S3 Fig). The post batch corrected data was reviewed (S8-15 Figs). Sex and smoking showed some separation and would need further investigation (S8 and S9 Figs). No separation could be seen for age, BMI, chronic disease history, previous INH used, duration of INH and alcohol use (S10-15 Figs). Using the paired design with blocking, accounted for the covariates effects by blocking on the effect of each individual and are discussed below.

Model design

For the analysis we used a paired design and created the model with subject IDs (for blocking in a paired design), group (HITTIN and HIT), time of infection (1 and 6h) and *Mtb* infection status (uninfected and infected) as factors in the model using model.matrix from the stats package (v4.0.3).

In the individual blocking, individuals were defined per timepoint, due to large variance introduced to each individual due to time effect (Figs 7 and 8). The three factors group, time of infection and *Mtb* infection status were grouped together as a single interaction term and was modelled with the subject effect as a means model:

$$E(Gi)_{Model1} \sim \beta_0 + \sum_{j=1}^{n} \beta_{jkl}\, x_j + \beta_{Hkl}.x_{Hkl} + \beta_{Nkl}\,.x_{Nkl} + \epsilon$$

Where Gi is the log2(CPM) expression for each gene i (n = 14602) and E(Gi) is the expected gene expression. β_0 represents the intercept. βjkl represents the mean expression for each individual j (j=1 to total of n) at time k (k= 1h or 6h) for *Mtb* infection state l (l= uninfected or infected). H represents HIT and N represents HITTIN. xj is a variable representing the n samples in the data. The β value is the mean expression for each specified group after blocking on the individual averages. ϵ is the residual term and is assumed to be normally distributed with a constant variance across the range of data.

Contrasts were made using makeContrasts and defined as:

i) Group specific effects at 1h infected

ii) Group specific effects at 6h infected

iii) Differential response between groups at 1h infected

$(\beta_{HITTIN1inf}) - (\beta_{HIT1inf})$

iv) Differential response between groups at 6h infected

$(\beta_{HITTIN6inf}) - (\beta_{HIT6inf})$

Linear models were fitted with lmFit and eBayes to calculate the gene-wise test statistics (moderated t-statistic, p-values and B-statistic). Criteria for DEGs was defined by a Benjamini Hochberg FDR procedure as genes with an absolute logFC ≥ 0.2 and adjusted p value ≤ 0.05.

DEGs were used in a gene set enrichment analysis for pathways and Gene ontology (GO) enrichment using ReactomePA v1.34.0 and clusterProfiler v3.18.1 (84). enrichGO was used to test GO biological process, enrichKEGG for KEGG pathways and Reactome with enrichPathway. An FDR ≤ 0.1 was used for Benjamini- Hochberg's multiple testing correction. Pathways and GO terms with less than five assigned genes were excluded.

Flow data analysis

CD15+CD66b+ and CD15-CD66b- cells were calculated as a percentage of total CD45+ single cells. Each subset CD15+CD66b+ and CD15-CD66b- was then further stratified into the relevant subpopulation contribution, which were then expressed as a percentage of each subset. CD15+CD66b+ was stratified as CD16+ (neutrophils) and CD16-$CD14_{low}$ (eosinophils), and CD15-CD66b- into CD3+ (T-cells), CD3- CD14+ (Monocytes) and CD3- CD14- (Other). Wilcoxon rank sum test was used to calculated if there was a significant ($p<0.05$) difference in the median percentage contribution of each subset in HITTIN vs HIT using GraphPad Prism 8.0.1 (Supplementary Table 2).

Confocal Image analysis

Image from total of 9 HITTIN and 5 HIT neutrophil were included in the final analysis. Results of the Hoechst cell nuclei area count as well as the total NETs area (chromatin channel) were analysed in R studio. The log ratio of total nuclei area (Hoechst channel) at 6h to 1h was used to compare the infection effect of *Mtb* between and within groups on the change in area of cells (as a proxy for cell counts, since masking often under or overestimated cell counts, especially with neutrophil nuclei with trinucleate structures and cell clumps) over 1h to 6h (Fig 5i, S1 Fig). The total NET area change was determined by the total NET area (chromatin channel) to the total cell area (Hoechst channel) as determined for each timepoint and non-infection or infection with *Mtb*. To investigate if there is a difference in NET area change from 1h to 6h between PMN_{HITTIN} and PMN_{HIT} in response to infection, we calculated the log transformed ratio of the NET area change at 6h to 1h in uninfected and *Mtb* infected for each subject (Fig 5ii, S1 Fig).

A two-way mixed ANOVA analysis approach was used with the phenotype group (HITTIN vs HIT) describing the between-subject factor and *Mtb* infection status (non-infected vs infected) the within subject factor. Assumptions of normality, homogeneity of variances and homogeneity of covariances were met. After the removal of the initial extreme outlier, there were still some 3 outliers in the remaining analysis. These outliers were not removed, and a

robust ANOVA was performed using the WRS2 package in R (85). Further pairwise comparisons were done between PMN_{HITTIN} and PMN_{HIT} for non-infection as well as infection with *Mtb*, using a pairwise t-test and Bonferroni adjusted p-values.

Acknowledgements

This study was approved by the Health Research Ethics Committee (HREC) of Stellenbosch University [S18/08/175(PhD)]. The ResisTB study was approved by the Health Research Ethics Committee (HREC) of Stellenbosch University [N16/03/033 and N16/03/033A] and the Faculty of Health Sciences Human Research Ethics Committee of the University of Cape Town [HREC 755/2016 and 702/2017]. Additional approval was obtained from the City of Cape Town and Western Cape government for access to the relevant clinics.

The work was funded by the South African Medical Research Council through its Division of Research Capacity Development under the SAMRC Clinician Researcher M.D PhD Development programme and the Walter and Eliza Hall Institute of Medical Research. The content of any Publications from any studies during this Degree are solely the responsibility of the authors and do not necessarily represent the official views of the South African Medical Research Council. This publication is supported by NeutroTB which is part of the EDCTP2 programme supported by the European Union (grant number TMA2018CDF-2353-NeutroTB). The views and opinions of authors expressed herein do not necessarily state or reflect those of EDCTP. RJW is supported by the Francis Crick Institute which is funded by Wellcome (CC2112), UKRI (CC2112) and CRUK (CC2112). He is also supported by Wellcome (203135). We acknowledge the support of the DSI-NRF Centre of Excellence for Biomedical Tuberculosis Research, South African Medical Research Council Centre for Tuberculosis Research, Division of Molecular Biology and Human Genetics, Faculty of Medicine and Health Sciences, Stellenbosch University, Cape Town, South Africa.

For the purposes of open access, the author has applied a CC-BY public copyright licence to any author accepted manuscript arising from this submission.

Special acknowledgement to Dr Tracey Jooste for her manuscript input as well as Dr Sihaam Boolay and Dr Nasiema Allie for laboratory assistance and support and Arturo Zychlinsky for kind supply of PL2/3 mAb.

References

1. WHO W. Global tuberculosis report 2022 [Internet]. 2022 [cited 2023 Mar 14]. Available from: https://www.who.int/publications-detail-redirect/9789240061729

2. Lawn SD, Wilkinson RJ. ART and prevention of HIV-associated tuberculosis. Lancet HIV. 2015 Jun;2(6):e221-222.

3. Houben RMGJ, Crampin AC, Ndhlovu R, Sonnenberg P, Godfrey-Faussett P, Haas WH, et al. Human immunodeficiency virus associated tuberculosis more often due to recent infection than reactivation of latent infection. Int J Tuberc Lung Dis. 2011 Jan 1;15(1):24–31.

4. Kroon EE, Kinnear CJ, Orlova M, Fischinger S, Shin S, Boolay S, et al. An observational study identifying highly tuberculosis-exposed, HIV-1-positive but persistently TB, tuberculin and IGRA negative persons with *M. tuberculosis* specific antibodies in Cape Town, South Africa. EBioMedicine. 2020 Nov 1;61:103053.

5. Verver S, Warren RM, Munch Z, Vynnycky E, van Helden PD, Richardson M, et al. Transmission of tuberculosis in a high incidence urban community in South Africa. Int J Epidemiol. 2004 Apr;33(2):351–7.

6. TB Statistics for South Africa | National & provincial [Internet]. TBFacts. [cited 2019 Oct 31]. Available from: https://tbfacts.org/tb-statistics-south-africa/

7. Blomgran R, Ernst JD. Lung Neutrophils Facilitate Activation of Naive Antigen-Specific CD4+ T Cells during *Mycobacterium tuberculosis* Infection. J. Immunol. 2011 Jun 15;186(12):7110–9.

8. Kisich KO, Higgins M, Diamond G, Heifets L. Tumor Necrosis Factor Alpha Stimulates Killing of *Mycobacterium tuberculosis* by Human Neutrophils. Infect Immun. 2002 Aug;70(8):4591–9.

9. Ellison MA, Gearheart CM, Porter CC, Ambruso DR. IFN-γ alters the expression of diverse immunity related genes in a cell culture model designed to represent maturing neutrophils. PLOS ONE. 2017 Oct 5;12(10):e0185956.

10. Jena P, Mohanty S, Mohanty T, Kallert S, Morgelin M, Lindstrøm T, et al. Azurophil Granule Proteins Constitute the Major Mycobactericidal Proteins in Human Neutrophils and Enhance the Killing of Mycobacteria in Macrophages. PLOS ONE. 2012 Dec 14;7(12):e50345.

11. Martineau AR, Newton SM, Wilkinson KA, Kampmann B, Hall BM, Nawroly N, et al. Neutrophil-mediated innate immune resistance to mycobacteria. J Clin Invest. 2007 Jul;117(7):1988–94.

12. Lowe DM, Demaret J, Bangani N, Nakiwala JK, Goliath R, Wilkinson KA, et al. Differential Effect of Viable Versus Necrotic Neutrophils on *Mycobacterium tuberculosis* Growth and Cytokine Induction in Whole Blood. Front Immunol. 2018; 9: 903. doi: 10.3389/fimmu.2018.00903

13. Subrahmanyam YV, Yamaga S, Prashar Y, Lee HH, Hoe NP, Kluger Y, et al. RNA expression patterns change dramatically in human neutrophils exposed to bacteria. Blood. 2001 Apr 15;97(8):2457–68.

14. Lakschevitz FS, Visser MB, Sun C, Glogauer M. Neutrophil transcriptional profile changes during transit from bone marrow to sites of inflammation. Cell. Mol. Immunol. 2014 Jun 9;12:53.

15. Kobayashi SD, Voyich JM, Braughton KR, DeLeo FR. Down-Regulation of Proinflammatory Capacity During Apoptosis in Human Polymorphonuclear Leukocytes. J Immunol. 2003 Mar 15;170(6):3357–68.

16. Kobayashi SD, Malachowa N, DeLeo FR. Influence of Microbes on Neutrophil Life and Death. Front Cell Infect Microbiol. 2017; 7: 159. doi: 10.3389/fcimb.2017.00159

17. Witko-Sarsat V, Pederzoli-Ribeil M, Hirsch E, Hirsh E, Sozzani S, Cassatella MA. Regulating neutrophil apoptosis: new players enter the game. Trends Immunol. 2011 Mar;32(3):117–24.

18. Dallenga T, Repnik U, Corleis B, Eich J, Reimer R, Griffiths GW, et al. *M. tuberculosis*-Induced Necrosis of Infected Neutrophils Promotes Bacterial Growth Following Phagocytosis by Macrophages. Cell Host Microbe. 2017 Oct 11;22(4):519-530.e3.

19. McHenry ML, Benchek P, Malone L, Nsereko M, Mayanja-Kizza H, Boom WH, et al. Resistance to TST/IGRA conversion in Uganda: Heritability and Genome-Wide Association Study. EBioMedicine. 2021 Dec;74:103727. doi:10.1016/j.ebiom.2021.103727.

20. Sørensen OE, Borregaard N. Neutrophil extracellular traps - the dark side of neutrophils. J Clin Invest. 2016 May 2;126(5):1612–20.

21. Brinkmann V, Reichard U, Goosmann C, Fauler B, Uhlemann Y, Weiss DS, et al. Neutrophil Extracellular Traps Kill Bacteria. Science. 2004 Mar 5;303(5663):1532–5.

22. Braian C, Hogea V, Stendahl O. *Mycobacterium tuberculosis*-Induced Neutrophil Extracellular Traps Activate Human Macrophages. J Innate Immun. 2013;5(6):591–602.

23. Ramos-Kichik V, Mondragón-Flores R, Mondragón-Castelán M, Gonzalez-Pozos S, Muñiz-Hernandez S, Rojas-Espinosa O, et al. Neutrophil extracellular traps are induced by *Mycobacterium tuberculosis*. Tuberculosis. 2009 Jan 1;89(1):29–37.

24. Sollberger G. Approaching Neutrophil Pyroptosis. J Mol Biol. 2022 Feb 28;434(4):167335.

25. Berry MPR, Graham CM, McNab FW, Xu Z, Bloch SAA, Oni T, et al. An interferon-inducible neutrophil-driven blood transcriptional signature in human tuberculosis. Nature. 2010 Aug;466(7309):973.

26. Dallenga T, Linnemann L, Paudyal B, Repnik U, Griffiths G, Schaible UE. Targeting neutrophils for host-directed therapy to treat tuberculosis. Int J Med Microbiol. 2018 Jan;308(1):142-147. doi: 10.1016/j.ijmm.2017.10.001.

27. Corleis B, Korbel D, Wilson R, Bylund J, Chee R, Schaible UE. Escape of *Mycobacterium tuberculosis* from oxidative killing by neutrophils. Cell Microbiol. 2012 Jul;14(7):1109–21.

28. Borkute RR, Woelke S, Pei G, Dorhoi A. Neutrophils in Tuberculosis: Cell Biology, Cellular Networking and Multitasking in Host Defense. Int J Mol Sci. 2021 Apr 30;22(9):4801.

29. Morgan MJ, Liu Z gang. Crosstalk of reactive oxygen species and NF-κB signaling. Cell Res. 2011 Jan;21(1):103–15.

30. Fuchs TA, Abed U, Goosmann C, Hurwitz R, Schulze I, Wahn V, et al. Novel cell death program leads to neutrophil extracellular traps. J Cell Biol. 2007 Jan 15;176(2):231–41.

31. Papayannopoulos V, Metzler KD, Hakkim A, Zychlinsky A. Neutrophil elastase and myeloperoxidase regulate the formation of neutrophil extracellular traps. J Cell Biol. 2010 Nov 1;191(3):677–91.

32. Fernandez-Marcos PJ, Nóbrega-Pereira S. NADPH: new oxygen for the ROS theory of aging. Oncotarget. 2016 Jul 20;7(32):50814–5.

33. Rosazza T, Warner J, Sollberger G. NET formation - mechanisms and how they relate to other cell death pathways. FEBS J. 2021 Jun;288(11):3334–50.

34. Poli V, Pui-Yan Ma V, Di Gioia M, Broggi A, Benamar M, Chen Q, et al. Zinc-dependent histone deacetylases drive neutrophil extracellular trap formation and potentiate local and systemic inflammation. iScience. 2021 Nov 19;24(11):103256.

35. Hamam HJ, Khan MA, Palaniyar N. Histone Acetylation Promotes Neutrophil Extracellular Trap Formation. Biomolecules. 2019 Jan 18;9(1):32.

36. Chen KW, Monteleone M, Boucher D, Sollberger G, Ramnath D, Condon ND, et al. Noncanonical inflammasome signaling elicits gasdermin D-dependent neutrophil extracellular traps. Sci Immunol. 2018 Aug 24;3(26):eaar6676.

37. Castanheira FVS, Kubes P. Neutrophils and NETs in modulating acute and chronic inflammation. Blood. 2019 May 16;133(20):2178–85.

38. Wang K, Sun Q, Zhong X, Zeng M, Zeng H, Shi X, et al. Structural Mechanism for GSDMD Targeting by Autoprocessed Caspases in Pyroptosis. Cell. 2020 Mar 5;180(5):941-955.e20.

39. McCracken JM, Allen LAH. Regulation of Human Neutrophil Apoptosis and Lifespan in Health and Disease. J Cell Death. 2014 May 8;7:15–23.

40. Leisching GR. Susceptibility to Tuberculosis Is Associated With PI3K-Dependent Increased Mobilization of Neutrophils. Front Immunol. 2018 Jul 17;9:1669. doi: 10.3389/fimmu.2018.01669

41. Sapey E, Greenwood H, Walton G, Mann E, Love A, Aaronson N, et al. Phosphoinositide 3-kinase inhibition restores neutrophil accuracy in the elderly: toward targeted treatments for immunosenescence. Blood. 2014 Jan 9;123(2):239–48.

42. Meier S, Seddon JA, Maasdorp E, Kleynhans L, du Plessis N, Loxton AG, et al. Neutrophil degranulation, NETosis and platelet degranulation pathway genes are co-induced in whole blood up to six months before tuberculosis diagnosis. PLOS ONE. 2022;17(12):e0278295.

43. Khan MA, Palaniyar N. Transcriptional firing helps to drive NETosis. Sci Rep. 2017 Feb 8;7(1):41749.

44. Jorch SK, Kubes P. An emerging role for neutrophil extracellular traps in noninfectious disease. Nat Med. 2017 Mar 7;23(3):279–87.

45. Ronchetti L, Boubaker NS, Barba M, Vici P, Gurtner A, Piaggio G. Neutrophil extracellular traps in cancer: not only catching microbes. J Exp Clin Cancer Res. 2021 Jul 14;40(1):231.

46. Liu Q, Wu S, Xue M, Sandford AJ, Wu J, Wang Y, et al. Heterozygote Advantage of the rs3794624 Polymorphism in *CYBA* for Resistance to Tuberculosis in Two Chinese Populations. Sci Rep. 2016 Nov 30;6:38213.

47. Juan-García J, García-García S, Guerra-Laso JM, Raposo-García S, Diez-Tascón C, Nebreda-Mayoral T, et al. In vitro infection with *Mycobacterium tuberculosis* induces a distinct immunological pattern in blood from healthy relatives of tuberculosis patients. Pathog Dis. 2017 Nov 30;75(8).

48. Zmijewski JW, Banerjee S, Bae H, Friggeri A, Lazarowski ER, Abraham E. Exposure to hydrogen peroxide induces oxidation and activation of AMP-activated protein kinase. J Biol Chem. 2010 Oct 22;285(43):33154–64.

49. Zmijewski JW, Lorne E, Zhao X, Tsuruta Y, Sha Y, Liu G, et al. Antiinflammatory effects of hydrogen peroxide in neutrophil activation and acute lung injury. Am J Respir Crit Care Med. 2009 Apr 15;179(8):694–704.

50. Park DW, Zmijewski JW. Mitochondrial Dysfunction and Immune Cell Metabolism in Sepsis. Infect Chemother. 2017 Mar;49(1):10–21.

51. Lopes F, Coelho FM, Costa VV, Vieira ÉLM, Sousa LP, Silva TA, et al. Resolution of neutrophilic inflammation by H2O2 in antigen-induced arthritis. Arthritis Rheum. 2011 Sep;63(9):2651–60.

52. Chelombitko MA. Role of Reactive Oxygen Species in Inflammation: A Minireview. Moscow Univ BiolSci Bull. 2018 Oct 1;73(4):199–202.

53. Nguyen GT, Green ER, Mecsas J. Neutrophils to the ROScue: Mechanisms of NADPH Oxidase Activation and Bacterial Resistance. Front Cell Infect Microbiol. 2017 Aug 25;7:373. doi: 10.3389/fcimb.2017.00373

54. Jiao L, Song J, Ding L, Liu T, Wu T, Zhang J, et al. A Novel Genetic Variation in *NCF2*, the Core Component of NADPH Oxidase, Contributes to the Susceptibility of Tuberculosis in Western Chinese Han Population. DNA Cell Biol. 2020 Jan;39(1):57–62.

55. Tall AR, Westerterp M. Inflammasomes, neutrophil extracellular traps, and cholesterol. J Lipid Res. 2019 Apr;60(4):721–7.

56. Kroon EE, Coussens AK, Kinnear C, Orlova M, Möller M, Seeger A, et al. Neutrophils: Innate Effectors of TB Resistance? Front Immunol. 2018;9:2637.

57. Daigo K, Hamakubo T. Host-protective effect of circulating pentraxin 3 (PTX3) and complex formation with neutrophil extracellular traps. Front Immunol. 2012 Dec 13;3:378.

58. Garratt LW. Current Understanding of the Neutrophil Transcriptome in Health and Disease. Cells. 2021 Sep 13;10(9):2406.

59. Yvan-Charvet L, Ng LG. Granulopoiesis and Neutrophil Homeostasis: A Metabolic, Daily Balancing Act. Trends Immunol. 2019 Jul;40(7):598–612.

60. Sheshachalam A, Srivastava N, Mitchell T, Lacy P, Eitzen G. Granule Protein Processing and Regulated Secretion in Neutrophils. Front Immunol. 2014 Sep 19;5:448. doi: 10.3389/fimmu.2014.00448

61. Seshadri C, Sedaghat N, Campo M, Peterson G, Wells RD, Olson GS, et al. Transcriptional networks are associated with resistance to *Mycobacterium tuberculosis* infection. PLOS ONE. 2017;12(4):e0175844.

62. Coussens AK, Wilkinson RJ, Martineau AR. Phenylbutyrate Is Bacteriostatic against *Mycobacterium tuberculosis* and Regulates the Macrophage Response to Infection, Synergistically with 25-Hydroxy-Vitamin D_3. PLOS Pathog. 2015 Jul 2;11(7):e1005007.

63. Schauer C, Janko C, Munoz LE, Zhao Y, Kienhöfer D, Frey B, et al. Aggregated neutrophil extracellular traps limit inflammation by degrading cytokines and chemokines. Nat Med. 2014 May;20(5):511–7.

64. Deng Y, Ye J, Luo Q, Huang Z, Peng Y, Xiong G, et al. Low-Density Granulocytes Are Elevated in Mycobacterial Infection and Associated with the Severity of Tuberculosis. PLOS ONE. 2016 Apr 13;11(4):e0153567.

65. La Manna MP, Orlando V, Paraboschi EM, Tamburini B, Di Carlo P, Cascio A, et al. *Mycobacterium tuberculosis* Drives Expansion of Low-Density Neutrophils Equipped With Regulatory Activities. Front Immunol. 2019; 10: 2761. doi: 10.3389/fimmu.2019.02761

66. Silvestre-Roig C, Hidalgo A, Soehnlein O. Neutrophil heterogeneity: implications for homeostasis and pathogenesis. Blood. 2016 May 5;127(18):2173–81.

67. Wood R, Liang H, Wu H, Middelkoop K, Oni T, Rangaka MX, et al. Changing prevalence of TB infection with increasing age in high TB burden townships in South Africa. Int J Tuberc Lung Dis. 2010 Apr;14(4):406–12.

68. Gallant CJ, Cobat A, Simkin L, Black GF, Stanley K, Hughes J, et al. The impact of age and sex on anti-mycobacterial immunity of children and adolescents in an area of high tuberculosis incidence. Int J Tuberc Lung Dis. 2010;14(8):952–8.

69. Losman MJ, Fasy TM, Novick KE, Monestier M. Monoclonal autoantibodies to subnucleosomes from a MRL/Mp(-)+/+ mouse. Oligoclonality of the antibody response and recognition of a determinant composed of histones H2A, H2B, and DNA. J Immunol. 1992 Mar 1;148(5):1561–9.

70. Brinkmann V, Goosmann C, Kühn LI, Zychlinsky A. Automatic quantification of in vitro NET formation. Front Immunol. 2013 Jan 9;3:413.

71. Knackstedt SL, Georgiadou A, Apel F, Abu-Abed U, Moxon CA, Cunnington AJ, et al. Neutrophil extracellular traps drive inflammatory pathogenesis in malaria. Sci Immunol. 2019 Oct 18;4(40):eaaw0336.

72. Andrews, S. Babraham Bioinformatics - FastQC A Quality Control tool for High Throughput Sequence Data [Internet]. 2010 [cited 2021 Aug 20]. Available from: https://www.bioinformatics.babraham.ac.uk/projects/fastqc/

73. Ewels P, Magnusson M, Lundin S, Käller M. MultiQC: summarize analysis results for multiple tools and samples in a single report. Bioinformatics. 2016 Oct 1;32(19):3047–8.

74. Parekh S, Ziegenhain C, Vieth B, Enard W, Hellmann I. The impact of amplification on differential expression analyses by RNA-seq. Sci Rep. 2016 May 9;6(1):25533.

75. Library C Digital Initiatives, University of Idaho. HTStream: A Toolkit for High Throughput Sequencing Analysis [Internet]. Theses and Dissertations Collection. [cited 2021 Aug 20]. Available from: https://www.lib.uidaho.edu/digital/etd/items/streett_idaho_0089n_11229.html

76. Zerbino DR, Achuthan P, Akanni W, Amode MR, Barrell D, Bhai J, et al. Ensembl 2018. Nucleic Acids Res. 2018 04;46(D1):D754–61.

77. Dobin A, Davis CA, Schlesinger F, Drenkow J, Zaleski C, Jha S, et al. STAR: ultrafast universal RNA-seq aligner. Bioinformatics. 2013 Jan 1;29(1):15–21.

78. Dobin A, Gingeras TR. Mapping RNA-seq Reads with STAR. Curr Protoc Bioinformatics. 2015 Sep 3;51:11.14.1-11.14.19.

79. R Core Team. R: a language and environment for statistical computing [Internet]. Vienna, Austria.: R Foundation for Statistical Computing. 2018 [cited 2019 Aug 30]. Available from: https://www.gbif.org/tool/81287/r-a-language-and-environment-for-statistical-computing

80. Zhang Y, Parmigiani G, Johnson WE. ComBat-seq: batch effect adjustment for RNA-seq count data. NAR Genom Bioinform. 2020 Sep;2(3):lqaa078.

81. Robinson MD, McCarthy DJ, Smyth GK. edgeR: a Bioconductor package for differential expression analysis of digital gene expression data. Bioinformatics. 2010 Jan 1;26(1):139–40.

82. Liu R, Holik AZ, Su S, Jansz N, Chen K, Leong HS, et al. Why weight? Modelling sample and observational level variability improves power in RNA-seq analyses. Nucleic Acids Res. 2015 Sep 3;43(15):e97.

83. Ritchie ME, Phipson B, Wu D, Hu Y, Law CW, Shi W, et al. limma powers differential expression analyses for RNA-sequencing and microarray studies. Nucleic Acids Res. 2015 Apr 20;43(7):e47.

84. Yu G, Wang LG, Han Y, He QY. clusterProfiler: an R package for comparing biological themes among gene clusters. OMICS. 2012 May;16(5):284–7.

85. Mair P, Wilcox R. Robust statistical methods in R using the WRS2 package. Behav Res Methods. 2020 Apr;52(2):464–88.

930 **Table 1: Participant characteristics**

Characteristic	HITTIN[a], N = 17[*]	HIT[b], N = 11[*]	p-value[**]
Age	43.71 (6.43)	44.09 (6.89)	0.9
Sex			0.6
Female	13 / 17 (76%)	10 / 11 (91%)	
Male	4 / 17 (24%)	1 / 11 (9.1%)	
Weight	75.81 (17.26)	84.09 (18.12)	0.3
(Missing)	1	0	
Height	1.63 (0.09)	1.67 (0.06)	0.2
BMI[c]	28.87 (7.38)	30.15 (5.70)	0.3
(Missing)	1	0	
Time on ART[d]			
More than 1 year	17 / 17 (100%)	11 / 11 (100%)	
CD4 prior to starting ART[d]			0.4
< 200 CD4+ cells/mm3	17 / 17 (100%)	10 / 11 (91%)	
Between 200-350 CD4+ cells/mm3	0 / 17 (0%)	1 / 11 (9.1%)	
Last CD4 prior to enrolment	557.76 (229.70)	486.73 (236.91)	0.5
Last VL[e]			0.9
≤100	4/ 17 (24%)	4 / 11 (36%)	
124	1 / 17 (5.9%)	0 / 11 (0%)	
LDL[f]	12 / 17 (71%)	7 / 11 (64%)	
Current IPT[g]	1 / 17 (5.9%)	0 / 11 (0%)	>0.9
Previous IPT treatment as per months of treatment			0.2
0	2 / 17 (12%)	3 / 11 (27%)	
2	0 / 17 (0%)	1 / 11 (9.1%)	
3	0 / 17 (0%)	0 / 11 (0%)	
4	0 / 17 (0%)	0 / 11 (0%)	
6	0 / 17 (0%)	2 / 11 (18%)	
12	10 / 17 (59%)	5 / 11 (45%)	
24	1 / 17 (5.9%)	0 / 11 (0%)	
36	3 / 17 (18%)	0 / 11 (0%)	
Current	1 / 17 (5.9%)	0 / 11 (0%)	
Chronic Illness	2 / 17 (12%)	3 / 11 (27%)	0.4
Alcohol Use	7 / 17 (41%)	2 / 11 (18%)	0.2
Smoker	2 / 17 (12%)	0 / 11 (0%)	0.5
Recreational Substance (Cannabis) use	0 / 17 (0%)	1 / 11 (9.1%)	0.4

[*]Mean (SD); n / N (%) [**]Wilcoxon rank sum test; Fisher's exact test

[a] HITTIN (HIV-1-infected persistently TB, tuberculin and IGRA negative), [b] HIT (HIV-1-infected IGRA positive tuberculin positive), [c] BMI (body mass index) was calculated as weight (kg)/height^2(m), [d] ART (antiretroviral therapy), [e] VL (viral load), [f] LDL (lower than detectable level), [g] IPT (Isoniazid preventive therapy)

931

932

933 **Table 2: Number of differentially expressed genes and their pathway and GO term**
934 **enrichment for PMN_{HITTIN} and PMN_{HIT} in response to *Mtb***

Contrast	DEGs[a]	# Genes FDR[b] ≤ 0.05	# combined terms	KEGG	Reactome	GO BP[c]
				FDR≤ 0.1	FDR ≤ 0.1	FDR ≤ 0.1
PMN_{HIT} [d] 1hour(h) infected vs uninfected	Total	109	209	32	12	165
	Upregulated	98	215	33	13	169
	Downregulated	11	0	0	0	0
PMN_{HITTIN} [e] 1h infected vs uninfected	Total	191	349	38	19	292
	Upregulated	151	383	40	20	323
	Downregulated	40	0	0	0	0
PMN_{HITTIN} - PMN_{HIT} 1h infected[f]	Total	0	0	0	0	0
	Upregulated	0	0	0	0	0
	Downregulated	0	0	0	0	0
PMN_{HIT} 6h hours infected vs uninfected	Total	7610	701	65	15	621
	Upregulated	3816	915	53	51	811
	Downregulated	3794	10	0	10	0
PMN_{HITTIN} 6h infected vs uninfected	Total	6654	498	51	16	431
	Upregulated	3106	769	54	30	685
	Downregulated	3548	7	0	6	1
PMN_{HITTIN} - PMN_{HIT} 6h infected[g]	Total[h]	2285	496	111	86	299
	Less Upregulated[i]	1217	719	48	55	616
	Less Downregulated[j]	1068	29	13	12	4

[a] DEGs (Differentially expressed genes), [b] FDR (false discovery rate), [c] GO BP (Gene Ontology Biological Processes), [d] PMN_{HIT} (HIV-1-infected IGRA positive tuberculin positive), [e] PMN_{HITTIN} (neutrophils from HIV-1-infected persistently TB, tuberculin and IGRA negative), [f] Refers to the interaction test looking at the difference in response to *Mtb* infection after 1h between PMN_{HITTIN} and PMN_{HIT}, [g] Refers to the interaction test looking at the difference in response to *Mtb* infection after 6h between PMN_{HITTIN} and PMN_{HIT}, [h] Refers to combined responses with significant positive and negative log2 fold change (log2FC) from the interaction test, [i, j] Refers to the negative[i] and positive[j] log2FC results from the interaction test

935
936
937
938
939
940
941
942

Table 3: Top significantly differentially expressed up- and downregulated genes of interest in the "Neutrophil Extracellular Trap Formation" KEGG pathway, at 6hr of *Mtb* infection between PMN_{HITTIN} and PMN_{HIT}

Ensembl gene ID	Gene	Log2FC after 6h *Mtb* infection			
		PMN_{HITTIN}[a]	PMN_{HIT}[b]	PMN_{HITTIN} x PMN_{HIT}[c]	adj.P.Val[d]
ENSG00000125730	*C3*	2,167	3,0342	-0,8672	7,24E-05
ENSG00000172232	*AZU1*	-0,2334	0,4615	-0,6949	0,0457
ENSG00000103569	*AQP9*	1,4303	1,9949	-0,5646	5,15E-05
ENSG00000165168	*CYBB*	0,603	1,0804	-0,4775	0,0003
ENSG00000109320	*NFKB1*	2,1359	2,6025	-0,4666	0,0089
ENSG00000169032	*MAP2K1*	0,5357	0,9572	-0,4216	0,0004
ENSG00000196954	*CASP4*	0,539	0,96	-0,421	0,0004
ENSG00000137462	*TLR2*	0,3467	0,7557	-0,409	0,0154
ENSG00000136869	*TLR4*	0,8416	1,2239	-0,3823	0,006
ENSG00000137752	*CASP1*	1,028	1,4004	-0,3724	0,0085
ENSG00000145675	*PIK3R1*	-0,1129	0,253	-0,3659	0,0182
ENSG00000197548	*ATG7*	1,4527	1,808	-0,3553	0,0094
ENSG00000051523	*CYBA*	0,9853	1,3244	-0,3391	0,0196
ENSG00000128340	*RAC2*	0,3795	0,6811	-0,3015	0,0012
ENSG00000116701	*NCF2*	-0,1042	0,1583	-0,2625	0,0073
ENSG00000197405	*C5AR1*	-0,2218	-0,0056	-0,2162	0,0258
ENSG00000105221	*AKT2*	-0,1992	-0,4116	0,2124	0,0123
ENSG00000075624	*ACTB*	-0,3289	-0,5483	0,2195	0,045
ENSG00000126934	*MAP2K2*	-0,2818	-0,5169	0,2351	0,0304
ENSG00000171608	*PIK3CD*	-0,0918	-0,3555	0,2637	0,0151
ENSG00000005844	*ITGAL*	-0,0544	-0,3497	0,2952	0,0005
ENSG00000113648	*MACROH2A1*	-1,2462	-1,5613	0,3151	0,0234
ENSG00000197943	*PLCG2*	-0,5073	-0,8366	0,3293	0,0007
ENSG00000166501	*PRKCB*	-0,4236	-0,758	0,3343	0,0005
ENSG00000116478	*HDAC1*	-0,1265	-0,505	0,3785	0,0011
ENSG00000159339	*PADI4*	-0,2054	-0,5956	0,3902	0,0007
ENSG00000171720	*HDAC3*	-0,4041	-0,81	0,4059	0,0004
ENSG00000100030	*MAPK1*	-0,6563	-1,0774	0,4211	0,0004
ENSG00000164032	*H2AZ1*	-0,2065	-0,6703	0,4638	0,0002
ENSG00000246705	*H2AJ*	0,0745	-0,3918	0,4663	0,0078
ENSG00000102882	*MAPK3*	-0,7807	-1,2548	0,474	0,0009
ENSG00000110876	*SELPLG*	-1,5235	-2,0183	0,4948	0,0153
ENSG00000068024	*HDAC4*	-0,3348	-0,8415	0,5067	5,05E-05
ENSG00000142208	*AKT1*	-0,4288	-0,9999	0,5711	3,15E-05
ENSG00000197837	*H4-16*	-0,0671	-0,6704	0,6033	0,0073
ENSG00000104518	*GSDMD*	-0,2606	-0,9556	0,6951	0,0004
ENSG00000277224	*H2BC7*	-0,6019	-1,6061	1,0041	0,0252

[a] The average log2FC *Mtb* infection compared to the uninfected response for neutrophils from HITTIN at 6h.
[b] The average log2FC *Mtb* infection compared to the uninfected response for neutrophils from HIT at 6h.
[c] The average log2FC response difference between neutrophils from HITTIN and HIT in response to *Mtb* infection at 6h (interaction test).
[d] The adjusted p-value after the Benjamini Hochberg correction for multiple testing for interaction test looking at the differential response of HITTIN to HIT at 6h infected ("**PMN_{HITTIN} x PMN_{HIT}**")
Significant genes were defined as genes with an absolute log2FC ≥ 0.2 and adjusted p value ≤ 0.05

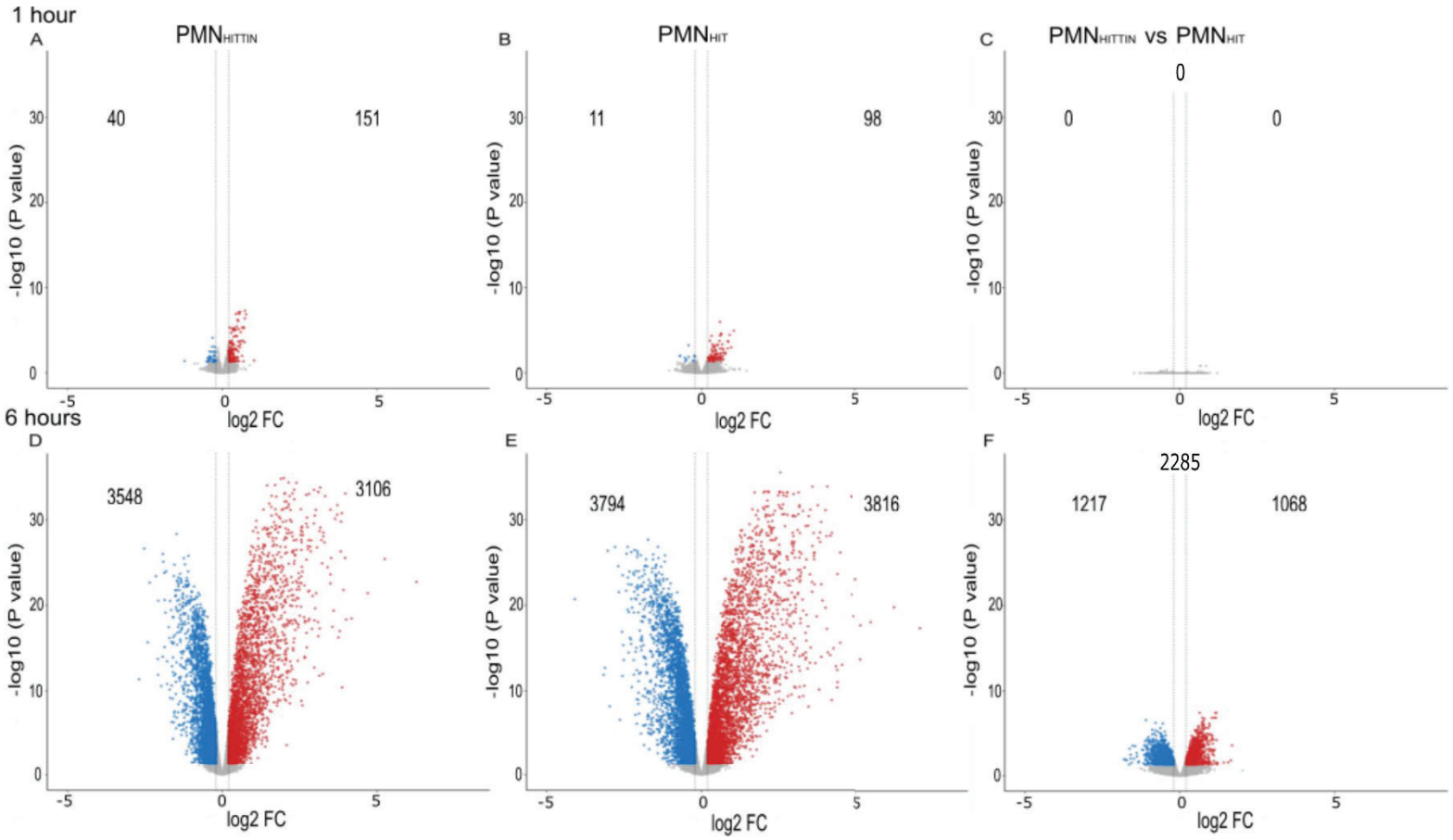

953

954 **Fig 1: Volcano plots of differential gene expression at 1h and 6h *Mtb* infection by PMN**
955 **from HITTIN and HIT**

956 Volcano plot for transcriptional responses to *Mtb* challenge for neutrophils from HITTIN (PMN_{HITTIN})
957 and HIT (PMN_{HIT}) participants at 1h **(A-C)** and 6h **(D-F)** post *Mtb* infection. The y-axis shows the
958 negative log10 unadjusted P value and the x-axis the log2 fold change (FC). The vertical dashed lines
959 represent log2FC thresholds of -0.02 and 0.02. Each gene is represented by a dot. Genes which are
960 downregulated or upregulated as determined by the FDR ≤ 5% are shown in blue and red,
961 respectively. Genes with non-significant expression changes and below the log 2FC threshold are
962 shown in grey. Differentially expressed genes at 1 h post-infection compared to 1h uninfected PMN
963 from HITTIN (PMN_{HITTIN}) **(A)** and HIT participants (PMN_{HIT}) **(B)**. Significant differentially triggered
964 genes between PMN_{HITTIN} and PMN_{HIT} at 1h post infection **(C)**. Differentially expressed genes at 6h
965 post-infection compared to 6h uninfected PMN from HITTIN (PMN_{HITTIN}) **(D)** and HIT participants
966 (PMN_{HIT}) **(E)**. Significant differentially triggered genes between PMN_{HITTIN} and PMN_{HIT} at 6h post
967 infection **(F)**.

968

969

970

971

972

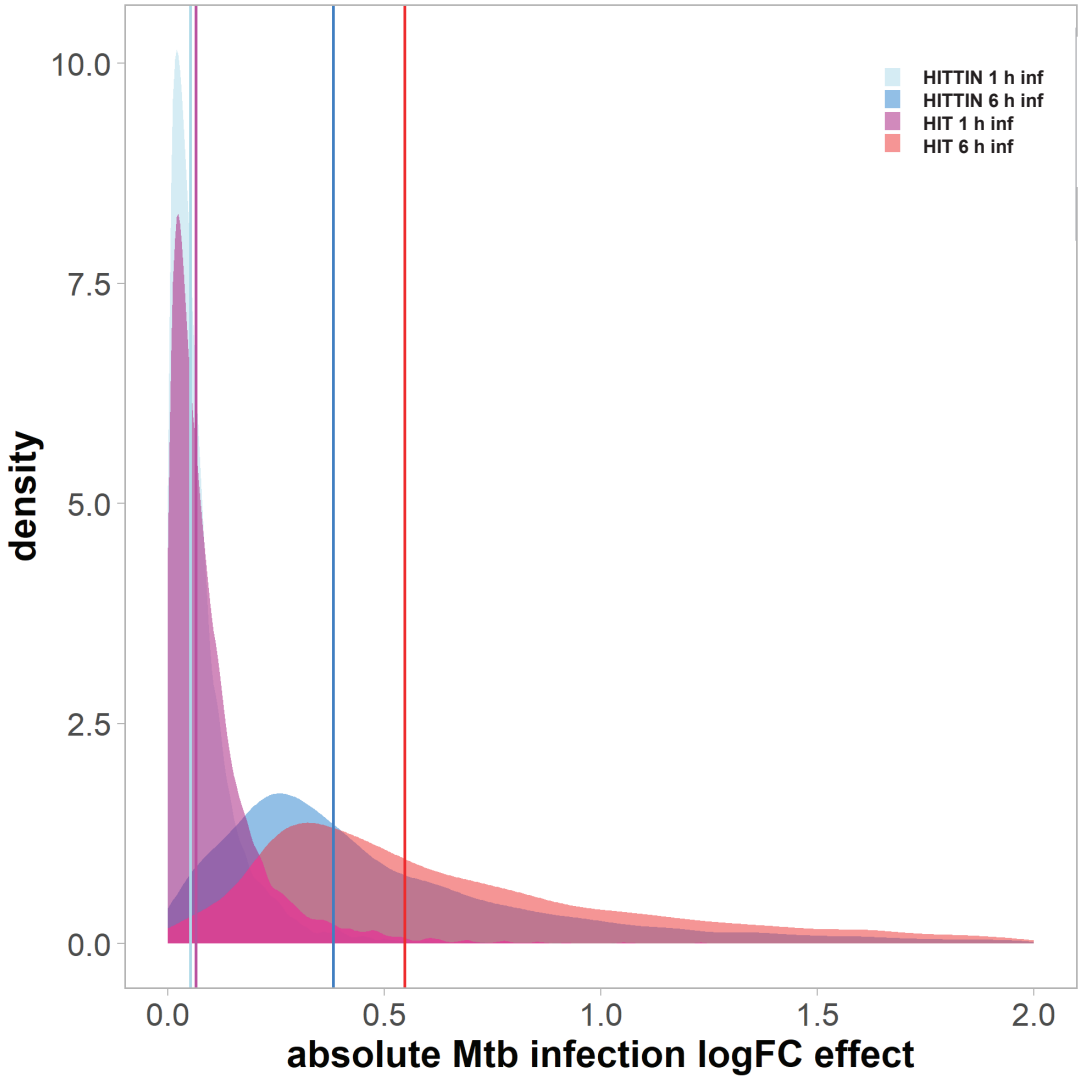

973

974 **Fig 2: The absolute log fold change *Mtb* infection effect at 1 and 6 h for PMN_{HITTIN} and**
975 **PMN_{HIT}**

976 The density plot shows the absolute log fold change (logFC) *Mtb* infection effect of each group at 1h
977 and 6h. All DEGs from Fig 1 had their logFC converted to absolute values and plotted using density
978 function. Absolute values for neutrophil DEGs from HITTIN participants are shown in light blue at 1h
979 and a darker blue at 6h. Absolute values for neutrophil DEGs from HIT participants are shown in
980 magenta at 1h and red at 6h. Vertical coloured lines indicate the mean of absolute values. PMN_{HITTIN}
981 show a lower logFC response to *Mtb* infection which is more pronounced at 6h compared to 1h of
982 infection with *Mtb*.

983

984

985

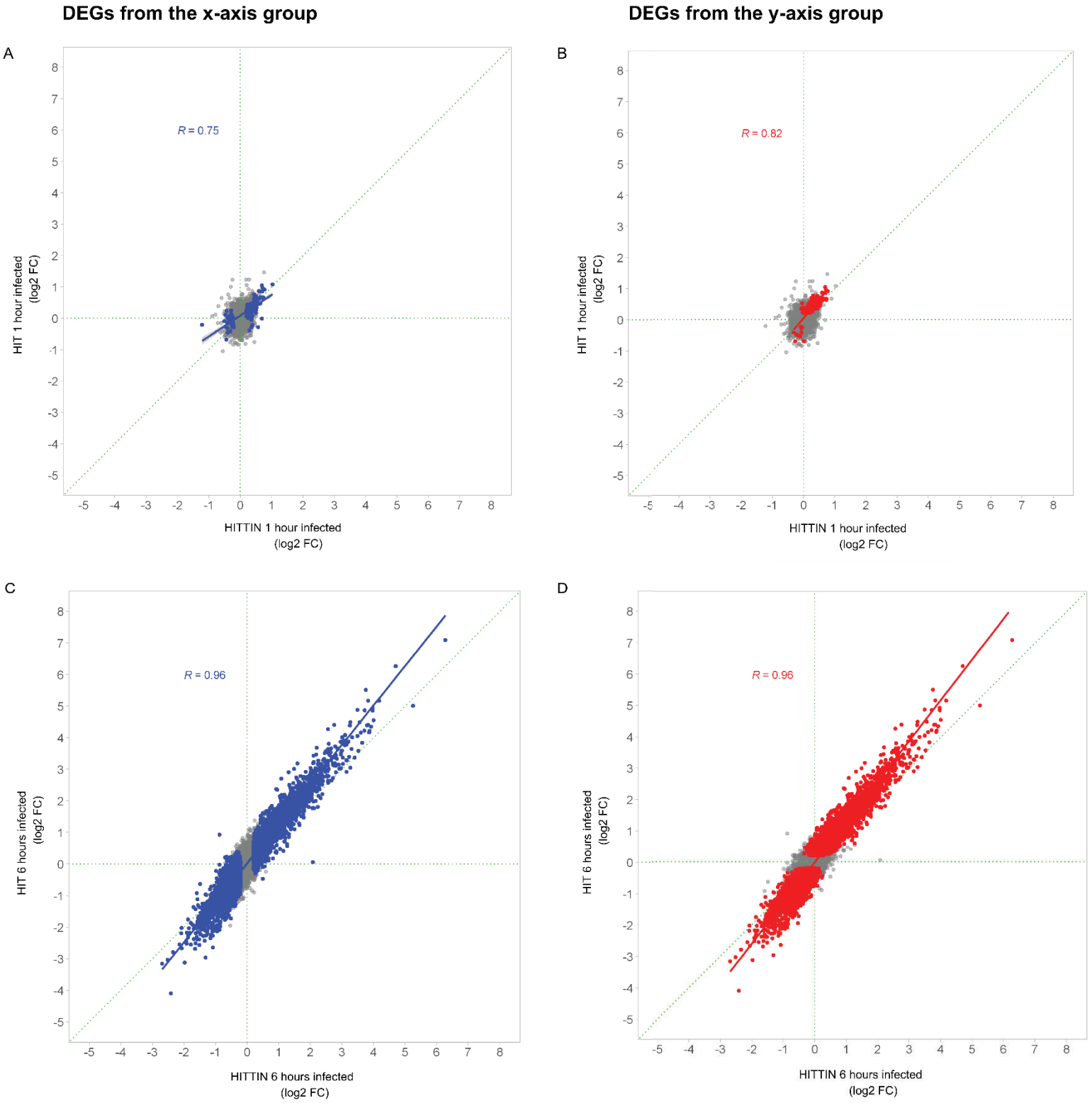

Fig 3: Correlation plots of log2FC gene expression after *Mtb* infection of PMN from HITTIN and HIT

"HITTIN 1h infected" represents the log2FC gene expression effect when comparing the 1h *Mtb* infection to the 1h uninfected response in neutrophils (PMN) from HIV-1-positive persistently TB, tuberculin and IGRA negative individuals (PMN_{HITTIN})(x-axis). "HITTIN 6h infected" is the same but for 6h. "HIT 1h infected" represents the log2FC gene expression effect when comparing the 1h Mtb infection to the 1h uninfected response in PMN from HIV-1-positive, IGRA positive, tuberculin positive

individuals (PMN_{HIT})(y-axis). "HIT 6h infected" is the same but for 6h. Scatterplots display the correlation of the log2FC gene expression as defined for each group at 1h **(A and B)** or 6h **(C and D)**. Each grey dot represents a differentially expressed gene (DEGs). The grey dots show combined DEGs from both groups represented on the x and y axis. Blue coloured dots indicate DEGs from the x-axis group and red dots indicate the y-axis group. Pearson correlation (R value) was calculated for the coloured DEGs. The log2FC for each group is plotted with the y-axis as the reference group. Differential gene expression is more pronounced in genes with the highest log2FC, with the majority of genes displaying good correlation between phenotype groups.

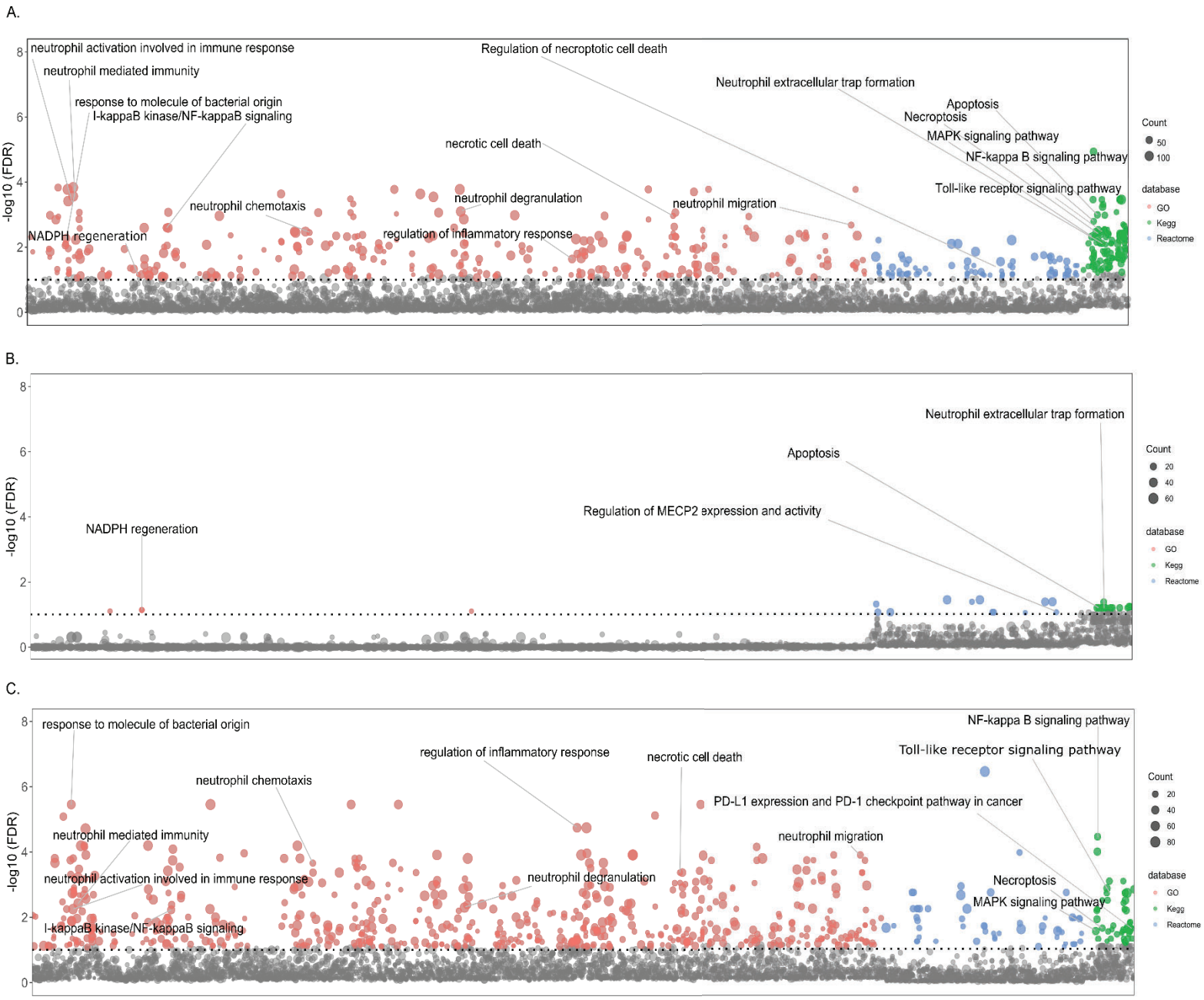

Fig 4: Manhattan plot for enrichment tests of GO terms and Kegg and Reactome pathways

The Manhattan plot shows pathways and GO terms for the DEGs triggered significantly differentially by *Mtb* in neutrophils from HITTIN versus neutrophils from HIT participants after 6h of infection. The tested terms are distributed along the x-axis. The y-axis represents the negative log 10 false discovery rate (FDR) result with the horizontal dotted line indicating the 10% FDR significance cut-off. Grey dots represent terms not meeting the significance threshold. Coloured dots represent significant terms from GO (red), Kegg (green) and Reactome (blue). The number of DEGs in each term is represented by the scaled size of the dot. Panel **(A)** shows the terms detected by all significantly different DEGs in the HITTIN vs HT contrast. Panel **(B)** shows significant terms which are driven by genes with significant positive FC/less downregulated by PMN from HITTIN participants while panel **(C)** displays terms for genes significantly less upregulated for PMN from HITTIN participants as compared to PMN_{HIT} after 6h of *Mtb* infection.

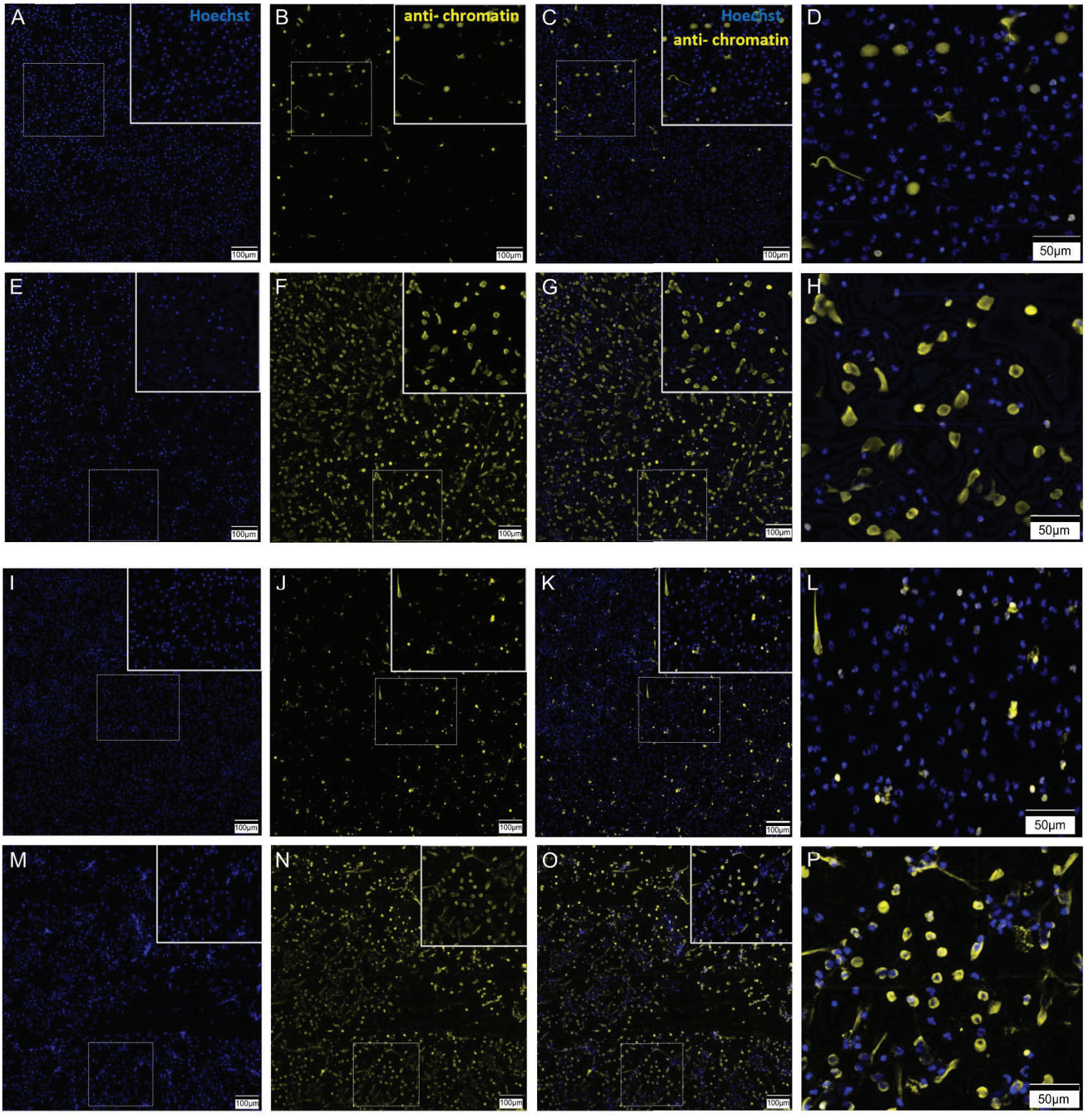

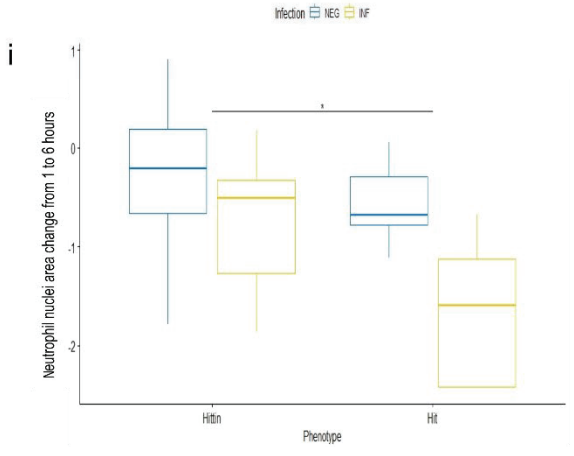

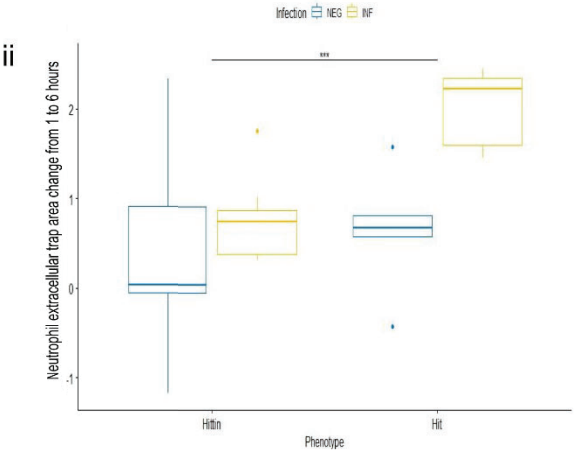

Fig 5: Representative images and quantification of the change in NET and nuclei area following *Mtb* infection of neutrophils from HITTIN and HIT.

PMN_{HTTIN} (A-H) and PMN_{HIT} (I-P) following Mtb infection for 1h (A-D and I-L) and 6h (E-H and M-P). *Mtb* infected neutrophils at 1h and 6h were stained with Hoechst 33342 **(A, E, I, M)** and PL2-3 **(B, F, J, N**). Overlap between the two stains is shown in (C, G , K ,O) with enlarged box panels in **(D, H, L, P**; blue, DNA; yellow, chromatin); **(i)** Boxplots for total log change in nuclei area (Hoescht stain, calculated as shown in S1 Fig) from 1h to 6h uninfected and infected with *Mtb* in HITTIN vs HIT. There was a significant *Mtb* infection effect, $F(1,12)=9.729$, $p=0.009$ with pairwise comparisons showing a significant difference between the total change in cell nuclei area from 1h to 6h after *Mtb* infection in HITTIN compared to HIT ($p=0.04$*, pairwise t-test), **(ii)** Boxplots for total log change in NET area (corrected for by the change in cell nuclei area, calculated as shown in S1 Fig) (PL2-3 anti-chromatin stain) from 1h to 6h uninfected and infected with *Mtb* in HITTIN vs HIT. There was a significant Mtb infection effect, $F(1, 10.5924) = 5.3398$, $p < 0.0421$ with pairwise comparisons showing a significantly difference between the total changed in cell nuclei area from 1h to 6h after *Mtb* infection in HITTIN compared to HIT ($p=0.0003$***, pairwise t-test). The scale bars represent 100 μm **(A-C, E-G, I-K, M-O)** and 50 μm **(D, H, L, P)**.